Offshore Low-trophic Aquaculture in Multi-Use Scenario Realisation

Grant agreement number: 101094065
Topic: HORIZON-MISS-2021-OCEAN-04-01
Starting date: 1 January 2023
Duration: 48 months

D3.2
Title: Report on assessment of carbon and nutrient uptake, and quantification of ecosystem services.

Date of delivery:
02.01.2026

Organization name of lead participant for this deliverable:
Institute of Marine Research

"Funded by the European Union, grant agreement NO 101094065. Views and opinions expressed are however those of the author(s) only and do not necessarily reflect those of the European Union or CINEA. Neither the European Union nor the granting authority can be held responsible for them."

Dissemination level		
PU	Public, fully open	x
Sen	Sensitive, limited under the conditions of the grant agreement (only for members of the consortium, incl the Commission Services)	

Deliverable number:	D.3.2
Deliverable title:	Report on assessment of carbon and nutrient uptake, and quantification of ecosystem services.
Work package:	3
Lead participant:	Institute of Marine Research

Authors

Name	Organisation	E-mail
Antonio Agüera Garcia*	Institute of Marine Research	antonio.aguera@hi.no
Marie Maar*	Aarhus University	mam@ecos.au.dk
Johannes Pein	Hereon	johannes.pein@hereon.de
Charlotte Clubley	Aarhus University	cclubley@ecos.au.dk
Jonne Kotta	University of Tartu	jonne.kotta@sea.ee
Janus Larsen	Aarhus University	janus@ecos.au.dk

*corresponding authors

Keywords

Production potential, environmental conditions, ecosystem models, dynamic energy budget, siting,

Review History				
Date	Version	Review Author	Organisation	E-mail
Dec 30th 2025	1.0	Øivind Strand	IMR	Oivind.strand@imr.no
Dec 30th 2025	1.0	Morten Skogen	IMR	Morten.skogen@imr.no

"Funded by the European Union, grant agreement NO 101094065. Views and opinions expressed are however those of the author(s) only and do not necessarily reflect those of the European Union or CINEA. Neither the European Union nor the granting authority can be held responsible for them."

Executive Summary

This deliverable from the OLAMUR WP3 provides a description of the modelling approaches applied to evaluate the cultivation of low trophic species in the OLAMUR sites. It extends and updates D3.1. by providing a validation of the models using site specific datasets. The other main aim of this deliverable is to provide further detail on the ecosystem services of the cultivation of low trophic species in the co-location sites and to demonstrate the use of the models to provide datasets on food provisioning (production potential), impacts on nutrient cycling (nutrient depletion, nutrient harvest), inorganic carbon capture and water clarity. These datasets will be available to be used in the WP2 micro siting tools and WP5 data portal.

"Funded by the European Union, grant agreement NO 101094065. Views and opinions expressed are however those of the author(s) only and do not necessarily reflect those of the European Union or CINEA. Neither the European Union nor the granting authority can be held responsible for them."

"Funded by the European Union, grant agreement NO 101094065. Views and opinions expressed are however those of the author(s) only and do not necessarily reflect those of the European Union or CINEA. Neither the European Union nor the granting authority can be held responsible for them."

1. Introduction

This deliverable has two main aims: i) expand on the deliverable 3.1 (production data sets) by providing an updated overview of the modelling approaches applied at the different OLAMUR case studies to assess production potential of low trophic species and ii) provide an evaluation of key ecosystem services provided by the cultivation of such species at the OLAMUR case studies areas. This deliverable provides datasets assessing the ecosystem services of the cultivation of low trophic species.

The cultivation of low trophic species provides essential benefits to humans; these ecosystem services are inherent to the cultivated species and relate directly to their biological activity and their function within ecosystems. This task focus on the following ecosystem services: food provisioning (production potential) and water quality regulation by their impact on nutrient cycling and primary productions.

Further, the developed models were used to compare the potential of the different pilots and relate this to their environmental particularities and their co use in different farming scenarios, including estimates of production carrying capacity.

In this report we provide a summary of the methodology: models applied, validation, scenarios run, outputs, and justification. The datasets produced in this deliverable will be transferred to WP5 to be added to the OLAMUR data portal and used in WP2 micro-siting tool. As such this deliverable update and extend the data provided by deliverable 3.1. while providing further details into models descriptions, validation and application to the study cases in the OLAMUR project.

2. Material & Methods

This task used local high resolution 3D ecological modeling for the pilot sites (SCHISM for pilot A, FlexSem for pilot B, and a box farm model for pilot C). The ecosystem models were coupled with existing Dynamic Energy Budget Individual Based Models (DEB IBM) for blue mussels, and in pilot C also for rainbow trout. New models were developed for the seaweeds sugar kelp and *Fucus*. The models were used to assess farm scale spatial production patterns, nutrient uptake, and impacts on primary production and water quality. Model outputs were validated against data gathered in the pilots (T1.4) and against oceanographic monitoring data from WP4 and/or monitoring stations. These models linked local environmental conditions with the physiological performance of the crop, allowing us to estimate spatial and temporal variability in crop status and their ecosystem services.

The modelling approach used is different for each study case, however for all study cases the aim is the same and the models are here used to produce datasets to evaluate the ecosystem services in the pilots and assess the suitability and limitations of the different locations and tools used.

The models applied in OLAMUR study cases are used here to assess the ecosystem services that relate directly to the biological/physiological activity of the low trophic species cultivated, more precisely this report provide insights on the services of food provisioning (production potential), impacts on nutrient and carbon cycling and water quality.

"Funded by the European Union, grant agreement NO 101094065. Views and opinions expressed are however those of the author(s) only and do not necessarily reflect those of the European Union or CINEA. Neither the European Union nor the granting authority can be held responsible for them."

2.1. Case study A: German Bight: Meerwind Süd-Ost

2.1.1. Description of modelling approach

To estimate aquaculture production in the area of case study A, we use an extension of the Semi-implicit Cross-scale Hydroscience Integrated System Model (SCHISM, Zhang et al. 2016) coupled via the Framework for Aquatic Biogeochemical Models (FABM, Bruggeman and Bolding, 2014) with the ECOSystem Model (ECOSMO, Daewel and Schrum 2013) modelling framework (in the following "SCHISM-FABM-ECOSMO", see Pein et al., 2021; Pein and Staneva, 2024), which integrates existing DEB model of blue mussels (Maar et al., 2009; 2023). The modelling strategy for resolving the technical structures of the offshore wind farm in case study A is based on explicit resolution of the monopiles. The 80 monopiles of the wind farm *Meerwind Süd | Ost* were inserted into an existing model grid (Pein et al., 2023) and thus extend the high-resolution region north of Helgoland with minimum side lengths of the mesh cells of 2.5 m to the wind farm foundations. The aquaculture variables can be initialised anywhere within the model domain including very close or in between the monopile foundations.

The modelling framework is based on the hydrodynamic core of the SCHISM model (Zhang et al., 2016). SCHISM solves the Reynolds-averaged Navier-Stokes equations on an unstructured grid and is characterised by robust and efficient solution algorithms that make it possible to calculate complex coupled models in model areas with sometimes very high resolution over relevant time periods. The validated ecosystem model ECOSMO (Schrum et al., 2006; Daewel and Schrum 2013) is coupled with SCHISM via the coupling interface FABM (Bruggeman and Bolding, 2014). The model system was further adapted to the real dynamics in the offshore area by coupling the hydrodynamic module with a module for wind waves (WWM - Roland et al., 2012). The integration of wind wave dynamics into the numerical was important to set realistic vertical mixing in the offshore environment and allow for windfarm monopile structures represented in the numerical mesh to have local impact such as wind wave attenuation (Hosseini et al., 2025). The forcing strategy and parametrising were adopted following the latter publication.

The integrated model system physics-ecology-aquaculture described here was developed during the reporting period based on the existing model framework SCHISM-FABM-ECOSMO and existing F90 and XML codes of blue mussel dynamics from other models (Maar et al. 2009, 2023). To enable integration with the latest and most sophisticated SCHISM and FABM versions, further adjustments were made to the code. The complete modelling framework physics-ecology plus DEB mussel model was run in a semi-coupled mode with mussel growth depending on the Chl *a* availability but with the depletion of Chl *a*. This approach was chosen to assess the growth and harvest potential at the site using different parametrization from the literature. For the scenario exercises, namelist parameters reported by Buer et al. (2020) were adopted. The two-coupling with depletion of phytoplankton by the mussel is technically accomplished and will be presented in the next deliverable.

"Funded by the European Union, grant agreement NO 101094065. Views and opinions expressed are however those of the author(s) only and do not necessarily reflect those of the European Union or CINEA. Neither the European Union nor the granting authority can be held responsible for them."

The model area of the southern North Sea and the German estuaries allows extensive flexibility in the choice of oceanic forcing (Fig. 2.1). Here, the physical re-analyses available via CMEMS based on the AMM15 model were used for the forcing of water levels, salinity, temperature and horizontal velocities. These data have hourly resolutions and are therefore tide-resolving. The atmospheric forcing is based on the ERA5 re-analyses of the European Centre of Medium-Range Weather Forecasts (Hersbach et al., 2020). The discharges of seven major rivers around the southern North Sea, including the Rhine, Ems, Weser and Elbe, were compiled from raw data from the Waterways Administration and processed data (kindly provided by S. van Leeuwen, NIOZ). The same applies to the nutrient concentrations of the contributories.

2.1.2. Model validation

Validation of environmental parameters.

The physical-biogeochemical coupled model, which serves as the basis for the coupling with the DEB model, was calibrated and validated for the year 2020 when data coverage in the southern North Sea was acceptable. The simulated phytoplankton quantity is of crucial importance for realistic forcing of aquaculture of lower trophic levels. Therefore, realistic simulation of dissolved chlorophyll-a was given the highest priority during calibration and validation. Due to the significant variations observed among different satellite products, priority was given to validation against in situ data (source: ICES, https://www.ices.dk/data/dataset-collections/pages/default.aspx). The blue mussel DEB model was also validated using field data of case study A from WP1. Two sampling dates (May and August) provided data on mussel growth at the Case A location.

2.1.3. Run scenarios

A screening scenario ("M0") to assess the harvest potential of mussels within the modelled area was performed, this run disregards the feedback from the aquaculture module on the biogeochemical simulation, in this way farms in neighbouring cells do not influence each other through depletion of food and the maximun biomass of mussels can be assessed. Additionally three realistic scenarios with feedback were performed. In scenario "M1", a single farm is located in the area of the experimental farm in WP1 Case Study A, in the south-eastern part of the *Meerwind* wind farm. The 'M2' and 'M3' scenarios involve the even distribution of farms across a rectangular grid, with an average distance of 350 metres ("M2") and 700 metres ("M3"), respectively. In all scenarios, blue mussels were initialized at the farm sites in May whereas the harvest potential in terms of farm biomass was assessed at the end of December. In all scenarios the vertical farm extension was assumed to be ~5 m. The model domain with the location and configuration of monopiles of the Meerwind offshore windfarm are illustrated in Fig. 2.1.1. In the same figure, a sketch of the smart farm and marker buoys inside the farm set up by WP1/Case study A is given, whereas the marker buoys served as substrate for blue mussels to be sampled during the project.

"Funded by the European Union, grant agreement NO 101094065. Views and opinions expressed are however those of the author(s) only and do not necessarily reflect those of the European Union or CINEA. Neither the European Union nor the granting authority can be held responsible for them."

Table 2.1.1. *Overview of model scenarios, with mussel farms placed as increasing distance form one another.*

Scenario	Description	Feedback to BGM
M	Farms in all cells	x
M1	Farm placed only in pilot farm location	✓
M2	Farms placed 350m distant from one another	✓
M3	Farms placed 700m distant from one another	✓

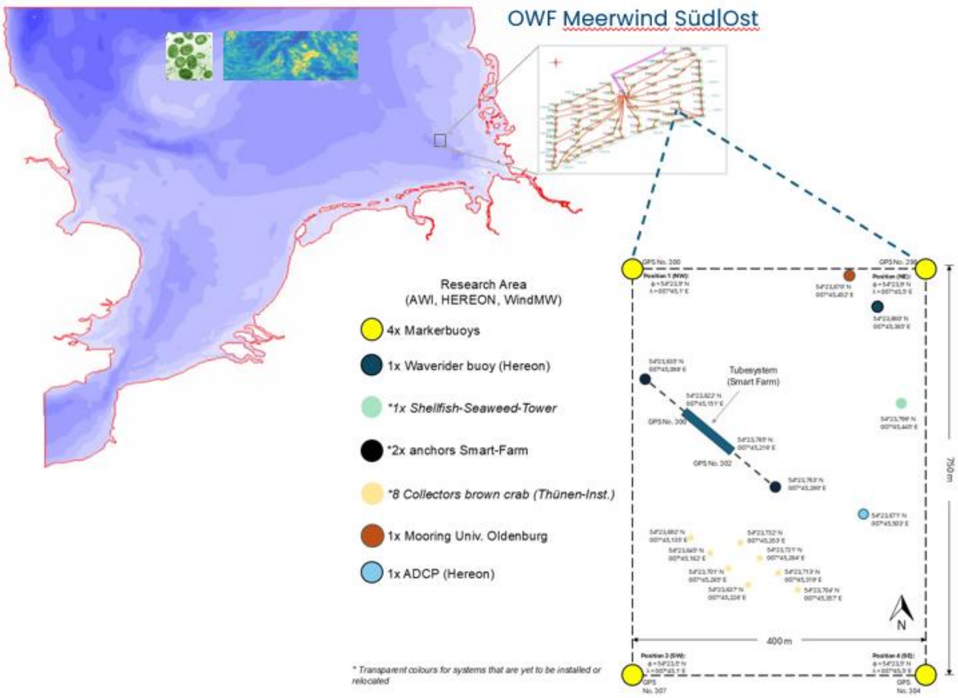

Figure 2.1.1. *Illustration of the model domain of the coupled physical-biogeochemical model with a schematic of the offshore windfarm Meerwind Süd|Ost and a diagram indicating the position of marker buoys and experimental aquaculture installations (i.e. Smart Farm) in WP1/Case study A, that serve here as siting example for the minimal scenario "M1".*

The scenarios M1-M3 were also used to quantify the ecosystem services provided by the lower-trophic level aquaculture as simulated by the modelling framework. The ecosystem services with a direct impact on the surrounding ocean provided by low-trophic-level aquaculture include the reduction of nutrients and suspended solids. This is the primary means of mitigating the effects of eutrophication, potentially resulting in increased oxygen concentrations. The non-linear nature of the interactions between physics, biogeochemistry and low-trophic level aquaculture require a numerical model coupling these compartments at the model time step level which is 1 minute here. Thus, coupled model system SCHISM-(FABM)-ECOSMO-DEB (mussel) used here can map the ecosystem services through the feedback of the aquaculture module (DEBmussel) to the ecosystem module (ECOSMO), i.e., through the fact that mussel growth locally removes phytoplankton from the ecosystem.

"Funded by the European Union, grant agreement NO 101094065. Views and opinions expressed are however those of the author(s) only and do not necessarily reflect those of the European Union or CINEA. Neither the European Union nor the granting authority can be held responsible for them."

2.2. Case study B: Danish Kriegers Flak

2.2.1. Description of modelling approach

Study area

Kriegers Flak is a reef located in the central Arkona Basin in the Western Baltic Sea, where European energy company Vattenfall runs an offshore wind farm consisting of 72 turbines (area: 132 km^2; Figure 2.2.1). Within the Kriegers Flak offshore wind farm, a pilot farm composed of four long lines, two growing mussels (*Mytilus* spp.) and two growing sugar kelp (*Saccharina latissima*), is present between the turbines in the south-eastern corner (Figure 2.2.1; WP1). The mussel lines were deployed in May 2024, whilst there have been two growing seasons for the sugar kelp, deployed in November 2023 and again in 2024.

Model system

At the Kriegers Flak case study site, the potential for multi-use of the Kriegers Flak offshore wind farm with low-trophic aquaculture of mussels and kelp is being evaluated by dynamic models simulating the growth, nutrient uptake, and carbon storage of these two species, using the FlexSem model framework (Larsen et al. 2020, Larsen 2024). These models are fully coupled to a 3D biogeochemical model, which is one-way coupled to a hydrodynamic model. The nonhydrostatic hydrodynamic setup in FlexSem uses a computational mesh which varies in horizontal resolution from 343 m within the offshore wind farm to 1,654 m in the area outside of the wind farm.

The model has a circular open boundary broken only by the easternmost point of the island of Møn, Denmark (Figure 2.2.1). Open boundary conditions and initial fields for both hydrodynamics and biogeochemistry were interpolated from a previous run of FlexSem for the Inner Danish Waters (see https://marweb.bios.au.dk/flexsem/models/models.aspx?menu=idw for details). Maximum water depth in the model set up for Kriegers Flak is 40 m, separated into 19 layers: seven 1 m layers in the upper 7 m, nine 2 m layers from 7-25 m, and three 5 m layers from 25-40 m. The model has a total of 56,310 computational cells. Meteorological forcings were interpolated from WRF model version 3 output provided by the Danish Technical University (DTU). This included current wind turbines in the area and the associated wind wake. The physical effects from monopiles were added as drag and turbulent kinetic energy (Rennau et al. 2012). The model has a timestep of 120 seconds and covers the year 2019.

"Funded by the European Union, grant agreement NO 101094065. Views and opinions expressed are however those of the author(s) only and do not necessarily reflect those of the European Union or CINEA. Neither the European Union nor the granting authority can be held responsible for them."

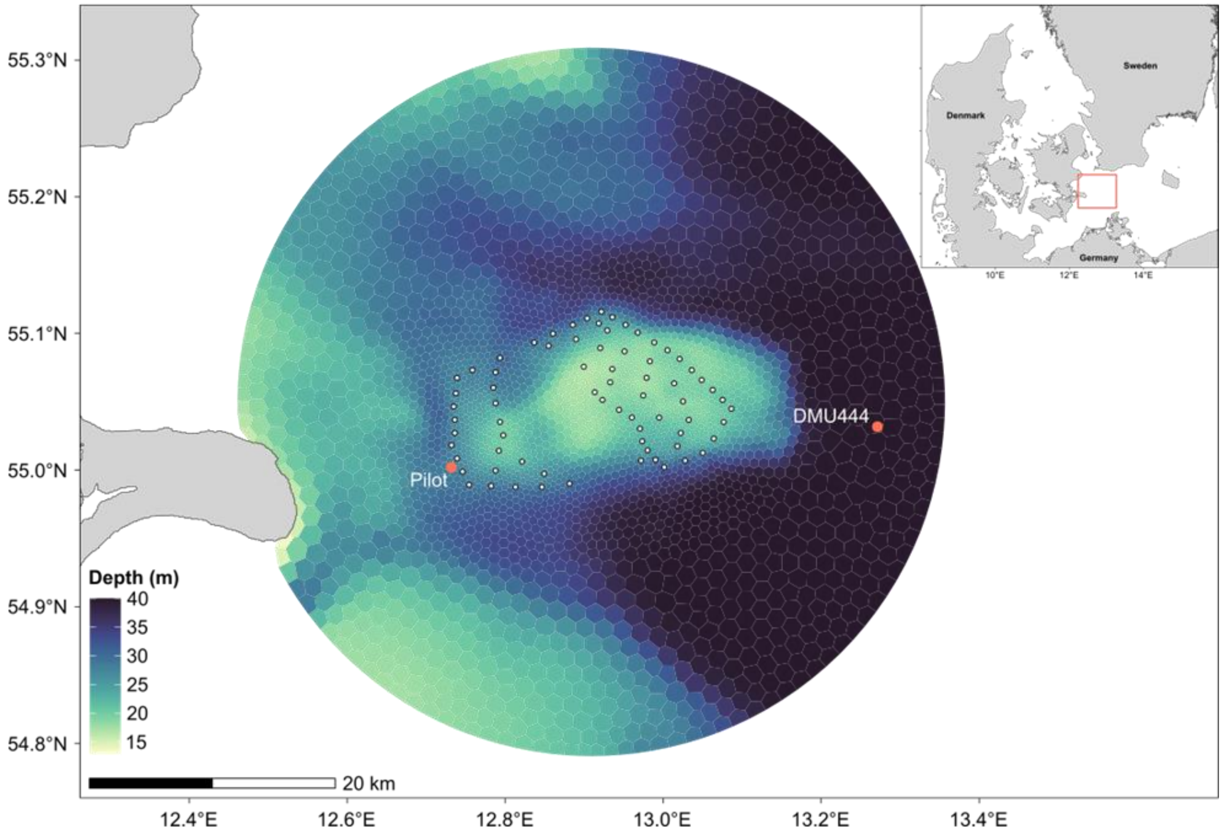

Figure 2.2.1. *Study area. The model domain showing bathymetry (m depth). White circles show the locations of the 72 wind farm pylons that make up Kriegers Flak offshore wind farm. Also shown is the location of the monitoring station DMU444, and the location of the pilot farm for mussel and kelp aquaculture (orange circles). Inset shows the location of Kriegers Flak in the Southern Baltic Sea (red box).*

Biogeochemical model

The biogeochemical model in FlexSem simulates changes in nutrients (NH_4, NO_3, PO_4), phytoplankton biomass, zooplankton biomass (meso- and microzooplankton), oxygen, detritus, and DON (labile and refractory dissolved organic nitrogen). The model estimates processes such as primary and secondary production, nutrient uptake, grazing, recycling of nutrients, excretion, respiration, growth, and mortality.

Mussel dynamic energy budget and nutrient removal model

The biogeochemical model is two-way coupled to a dynamic energy budget, individual based mussel growth model (DEB-IBM). The mussel model is based on a previously published model (Buer et al. 2020, Taylor et al. 2021, Maar et al. 2023, 2024). The mussel model tracks the biomass (g DW) and shell length (cm) of mussels over time as a function of temperature, salinity, and food (phytoplankton, microzooplankton, and detritus) concentration, as input from the biogeochemical model. There is feedback from the mussel DEB-IBM to the biogeochemical model through filtration of plankton, respiration (O_2), excretion (NH_4, PO_4), and faecal pellet production. Mussel farms were placed from 2 – 5 m depth, matching their deployment at the pilot farm. The mussel model was initialised on 1st July and harvested on 31st December the following year (1.5-year growth period).

Kelp production and nutrient removal model

"Funded by the European Union, grant agreement NO 101094065. Views and opinions expressed are however those of the author(s) only and do not necessarily reflect those of the European Union or CINEA. Neither the European Union nor the granting authority can be held responsible for them."

The biogeochemical model is two-way coupled to a kelp growth model based on that described and parameterised in Holst et al. (2025). The kelp model tracks the biomass of kelp (*M;* g-DW m-line^{-1} day^{-1}) as a function of the daily total of global irradiation:

$$\Delta M = \left(\alpha \times S_f\right) \times M_{CH_2O} \times I_{abs} - (r \times M)$$

α is the quantum yield (CO_2 quantum^{-1}); fixed CO_2 contributes to kelp biomass as glucose at a rate of 6 CO_2 per $C_6H_{12}O_6$$M_{CH_2O}$ = 30 g mol^{-1}I_{abs} is the daily total of light absorbed by the kelp canopy (mol-PAR m^{-1} d^{-1} . r is the base respiration rate of kelp (0.01 g-DW g-DW^{-1} d^{-1}; Holst et al. 2025. S_f (salinity, psu) in the Baltic Sea area on kelp growth, based on that described by Maar et al. (2023):

$$S_f(\alpha) = \left\{1\, for\, S \geq 25; 1 + \frac{S-25}{18} for\, 16 \leq S < 25; \frac{S}{32} for\, S < 16\right\}$$

We added nutrient (N and P) reserves of kelp to the model, loosely following the parameterisation of Broch and Slagstad (2012)'s dynamical model for *S. latissima* growth and Zollmann et al. (2021)'s *Ulva* sp. dynamic cultivation model. Nitrogen content in kelp reserves (N_r, g-N m^{-1}) was calculated at each timestep (Δt = 1 day) as:

$$N_r = N_r + \left(\left(N_{up} \times 0.014 \times M\right) - (r \times N_r)\right)\Delta t$$

Where the term $\left(N_{up} \times 0.014 \times M\right)$ describes the conversion of nitrogen uptake (N_{up}) from mmol-N g-DW^{-1} d^{-1} to g-N m^{-1} d^{-1}; and the term $(r \times N_r)$ describes the nitrogen lost through respiration. The uptake of DIN (NO_3 + NH_4), N_{up} (g-N m^{-1} d^{-1}), was parameterised as:

$$N_{up} = \left(\frac{N_{max} - N_f}{N_{max} - N_{min}}\right)\left(\frac{N_{up}^{max} \times DIN}{DIN + K_m}\right)$$

Where $N_r$is the nitrogen reserves (g-N m^{-1}) from eq. 1; N_{up}^{max} is the maximum N uptake rate (0.24 mmol-N g-DW^{-1} d^{-1}; Broch and Slagstad 2012); DIN is the inorganic nitrogen concentration of the surrounding waters (mmol m^{-3}); K_m is the uptake half saturation constant for nitrate (2 mmol m^{-3}; Jevne et al. 2020); N_{max} and N_{min} are the maximum (0.10 g-N g-DW^{-1}) and minimum (0.01 g-N g-DW^{-1}) N content of kelp, respectively (Boderskov et al. 2023); and N_f is the nitrogen content as a fraction of the standing stock dry weight (N_r/M ; g-N g-DW^{-1}).

The uptake of phosphorous (P_{up}; g-P m^{-1} d^{-1}) and the phosphorous content in the kelp (P_r; g-P m^{-1}) were calculated using the Redfield ratio N:P of 16:1.

The standing stock of kelp biomass (g-DW m^{-1}), M , was updated at each timestep (Δt = 1 day):

$$M \leftarrow M + \Delta M \times \Delta t \times N_{\lim it}$$

Where $N_{\lim it}$ describes the effect of nitrogen limitation on biomass production, parameterised as:

$$N_{\lim it} = \left\{\frac{\frac{N_f - N_{min}}{N_f}}{\frac{2 - N_{min}}{2}} for\, 2 \leq N_f;\ 1\, for\, N_f > 2\right\}$$

"Funded by the European Union, grant agreement NO 101094065. Views and opinions expressed are however those of the author(s) only and do not necessarily reflect those of the European Union or CINEA. Neither the European Union nor the granting authority can be held responsible for them."

The carbon content of kelp was calculated as 32% of total dry weight (M), based on previous studies by Bruhn et al. (2016), Nielsen et al. (2016), and Boderskov et al. (2023). Kelp farms were placed from 0 – 6 m depth. At the pilot farm kelp are grown to 15 m depth, but the biomass of kelp grown ≥ 6 m depth in the model was considered negligible. The kelp model was initialised on 1st January and harvested on 1st June. Later harvest was not possible due to settling of mussel spat on the crop at the pilot farm.

2.2.2. Model validation

Validation of environmental parameters

Environmental observations from the DMU444 monitoring station (Figure 2.2.1) in 2019 were extracted from the Danish National Database on Aquatic Monitoring for model validation. These observations were compared to model outputs for eight variables: surface temperature, surface salinity, surface nitrate, surface phosphate, surface Chl *a*, Secchi depth, and surface and bottom oxygen. Agreement between the model data and *in situ* observations was assessed by calculating Pearson's correlation coefficient (r) with a type II error of 5, normalised standard deviation (nSD), and a cost function (CF):

$$CF = \left| \frac{(\overline{m} - o)}{\sigma_o} \right|$$

Where $\overline{m}$ is the mean of model data; $\overline{o}$ is the mean of observational data; and σ_o is the standard deviation of the observational data (Radach and Moll 2006).

Validation of mussel DEB and nutrient removal model

Model results for mussel shell length (cm), individual dry weight (g ind^{-1}), biomass (kg FW m^{-1}), density (ind. m^{-1}), shell carbon content (g-C g-DW^{-1}), and nitrogen reserves (g-N g-DW^{-1}), were compared to measurements taken from the pilot farm at Kriegers Flak (WP1). Average values of measurements for each variable were available for two collector types, New Zealand and Bendler, on 28/08/24 and 19/02/25, and for the Bendler collector type only on 08/04/25 and 03/06/25. Data from the New Zealand collector were not available from the last two dates as the mussel farmer was unable to maintain these lines. Measurement dates and data availability are summarised in Table 2.2.1. All measurements were taken at 3 m depth from mussels deployed in 2024.

Table 2.2.1. *A summary of the available data from the Kriegers Flak pilot farm (WP1) for use in validating the mussel model. Data availability for the given date for the given collector type is indicated by × (no data available) or ✓ (data available).*

Measurement date	Collector type	Shell length (cm)	Individual dry weight (g)	Biomass (kg FW m^{-1})	Density (m^{-1})	Carbon (g-C g-DW^{-1})	Nitrogen (g-N g-DW^{-1})
28th Aug 2024	New Zealand	➲	✓	✓	×	×	×
	Bendler	×	×	✓	×	×	×
19th Feb 2025	New Zealand	➲	✓	✓	✓	×	×

"Funded by the European Union, grant agreement NO 101094065. Views and opinions expressed are however those of the author(s) only and do not necessarily reflect those of the European Union or CINEA. Neither the European Union nor the granting authority can be held responsible for them."

	Bender	➲	✓	✓	✓	×	×
8th Apr 2025	Bendler	➲	✓	✓	×	✓	✓
3rd Jun 2025	Bendler	➲	✓	✓	×	✓	✓

Average values for shell length, individual dry weight, biomass, density, shell carbon content, and N content were compared with model values from the day of the measurements. Due to insufficient data from the pilot farms, no formal analyses of model performance for biological parameters were conducted.

Validation of kelp production and nutrient removal model

Model results for kelp biomass (g DW m^{-1}), frond length (m), and nitrogen reserves (g N g-DW^{-1}) were compared to measurements taken form the pilot farm at Kriegers Flak (WP1). Kelp biomass data were available for two growth seasons. For kelp deployed in 2023, data were available for two strains of kelp: one from Middelfart, Denmark and one from Kiel, Germany. For each strain, there were two groups of kelp, one that had undergone adaptation to low salinities and one that had not, resulting in four average measurements for each sampling date: Middelfart salinity adapted, Middelfart non-adapted, Kiel salinity adapted, Kiel non-adapted. For these kelp, biomass data were available for only the Kiel strain, measured at 1 m depth, on 17/04/24, and for both strains, measured at 1 m, 3 m and 6 m depth, on 22/05/24. Length data were available for both strains, measured at 1 m depth, from 27/02/24 and 16/04/24. For kelp deployed in 2024, only the Middelfart strain was used due to no stock of the Kiel strain, and no kelp underwent adaptation to low salinities. For these kelp, data on the biomass, frond length, and nitrogen reserves taken at 1 m depth were available for 19/02/25 and 08/04/25. These data are summarised in Table 2.2.2.

Table 2.2.2. *A summary of the available data from the Kriegers Flak pilot farm (WP1) for use in validating the kelp model. Data availability for the given date for the given strain of kelp is indicated by × (no data available) or ✓ (data available).*

Deployment year	Measurement date	Strain of kelp	Salinity adapted?	Depth of measurements	Biomass (g DW m^{-1})	Frond length (m^{-1})	Nitrogen reserves (g N g-DW^{-1})
2023	27th Feb 2024	Kiel	No	1 m	×	✓	×
			Yes				
		Middelfart	No				
			Yes				
	16th Apr 2024	Kiel	No	1 m	×	✓	×
			Yes				
		Middelfart	No				
			Yes				
	17th Apr 2024	Kiel	No	1 m	✓	×	×
			Yes				
	22nd May 2024	Kiel	No	1 m, 3 m, 6 m	✓	×	×
			Yes				

"Funded by the European Union, grant agreement NO 101094065. Views and opinions expressed are however those of the author(s) only and do not necessarily reflect those of the European Union or CINEA. Neither the European Union nor the granting authority can be held responsible for them."

		Middelfart	No				
			Yes				
2024	19th Feb 2025	Middelfart	No	1 m	✓	✓	✓
	8th Apr 2025	Middelfart	No	1 m	✓	✓	✓

Average values for biomass, frond length and nitrogen content were compared with model values from the day of the measurements. There were no measurements of phosphorous content of kelp taken at the pilot farm, and therefore validation of phosphorous reserves was not possible. Due to insufficient data from the pilot farms, no formal analyses of model performance for biological parameters were conducted.

2.2.3. Run scenarios

A number of steps were conducted to assess the harvest potential and suitability of locations within the Kriegers Flak offshore wind farm for mussel and kelp aquaculture. The potential harvest of both species within the boundary of the wind farm turbines (+ 200 m buffer) was screened based on (i) the maximum food/nutrient fluxes, which assure a high food/nutrient supply and less risk of depletion, and (ii) the maximum potential biomass of mussels and kelp (no depletion considered). A model was run in which kelp and mussel farms were placed within every computational cell of the FlexSem model and no feedback to the biogeochemical model was included. In this way, farms in neighbouring cells do not influence each other through depletion of food/nutrients and the maximum potential biomass of both species can be assessed. From the model output, harvest potential was assessed based on spatial variability in food and nutrient supply and the biomass of mussels and kelp at the ends of their respective production periods.

In the low trophic aquaculture farms, depletion of nutrients and food will occur to a variable extent dependent on the food/nutrient flux by advection. A higher food/nutrient flux will support a higher growth rate of the focal species and therefore can be used as an indicator for farming potential. The daily average food flux (mg Chl *a* m^{-2} s^{-1}) for mussels from 2 – 5 m depth was estimated by multiplying food concentration (mg Chl *a* m^{-2}) by the current speed (m s^{-1}). Values were averaged across time from 1st January – 31st December, representing the production period for mussel culture covered by the model, to show spatiotemporal variability in food supply (Figure 2.2.2A). Similarly, the daily average nutrient flux (mmol N m^{-2} s^{-1}) from 0 – 6 m depth was estimated by multiplying DIN (mmol N m^{-2}) by the current speed. Values were averages across time from 1st January – 1st June, representing the production period for kelp covered by the model, to show spatiotemporal variability in nutrient supply (Figure 2.2.2B).

"Funded by the European Union, grant agreement NO 101094065. Views and opinions expressed are however those of the author(s) only and do not necessarily reflect those of the European Union or CINEA. Neither the European Union nor the granting authority can be held responsible for them."

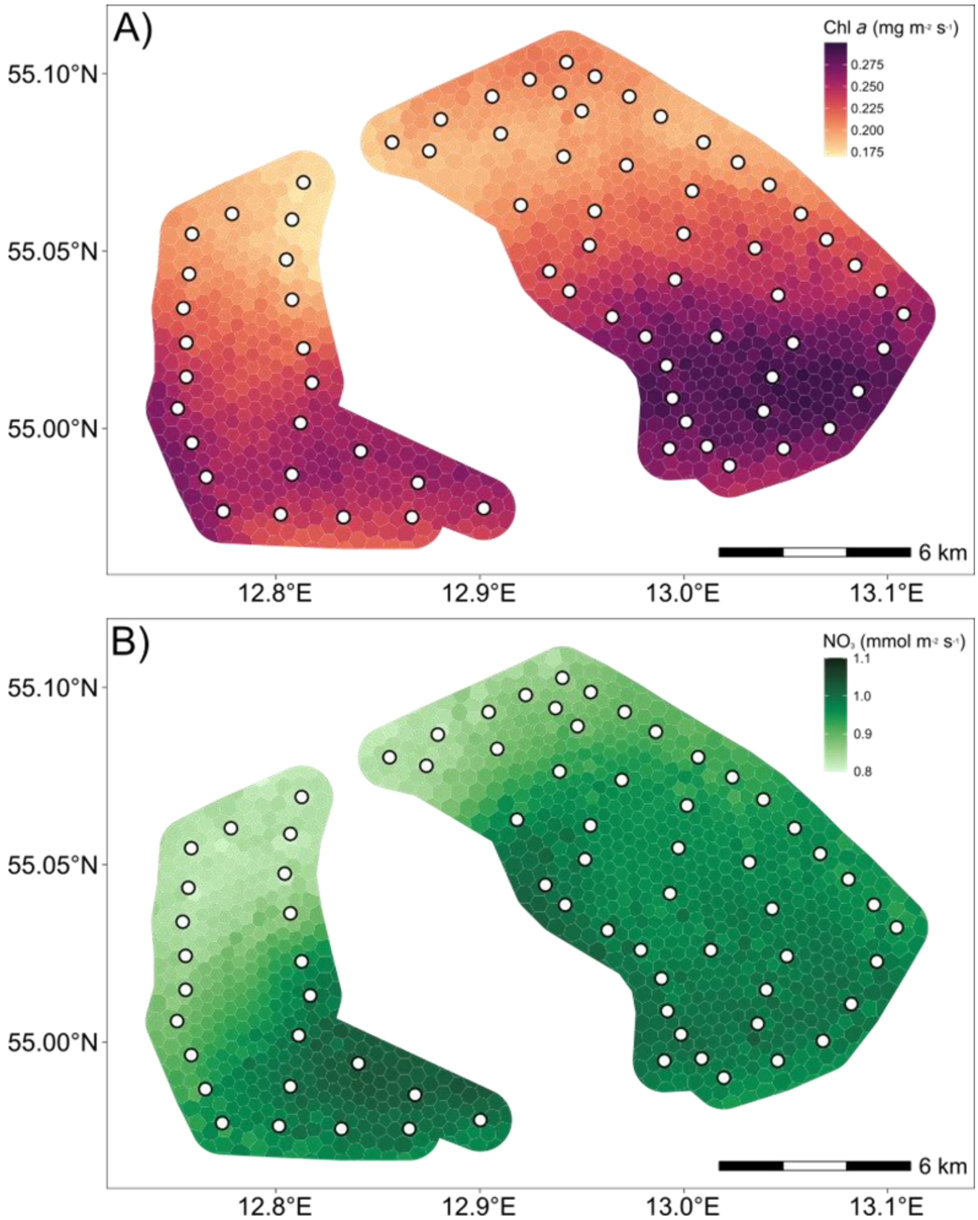

Figure 2.2.2. *Average food and nutrient flux within the boundary of the Kriegers Flak offshore wind farm. A) Average food flux (mg Chl a m^{-2} s^{-1}) over the period 1st January – 31st December 2019. B) Average nutrient flux (mmol NO_3 m^{-2} s^{-1}) over the period 1st January – 1st June 2019. White circles show the locations of the 72 wind turbines within the offshore wind farm.*

The maximum potential biomass of mussels and kelp was calculated as the biomass of both species on their respective 'harvest' dates. For mussels, model values for biomass (g DW) on the 31st December were summed from 2 – 5 m depth (Figure 2.2.3A). For kelp, model values for biomass (g DW) on the 1st June were summed from 0 – 6 m depth (Figure 2.2.3B).

"Funded by the European Union, grant agreement NO 101094065. Views and opinions expressed are however those of the author(s) only and do not necessarily reflect those of the European Union or CINEA. Neither the European Union nor the granting authority can be held responsible for them."

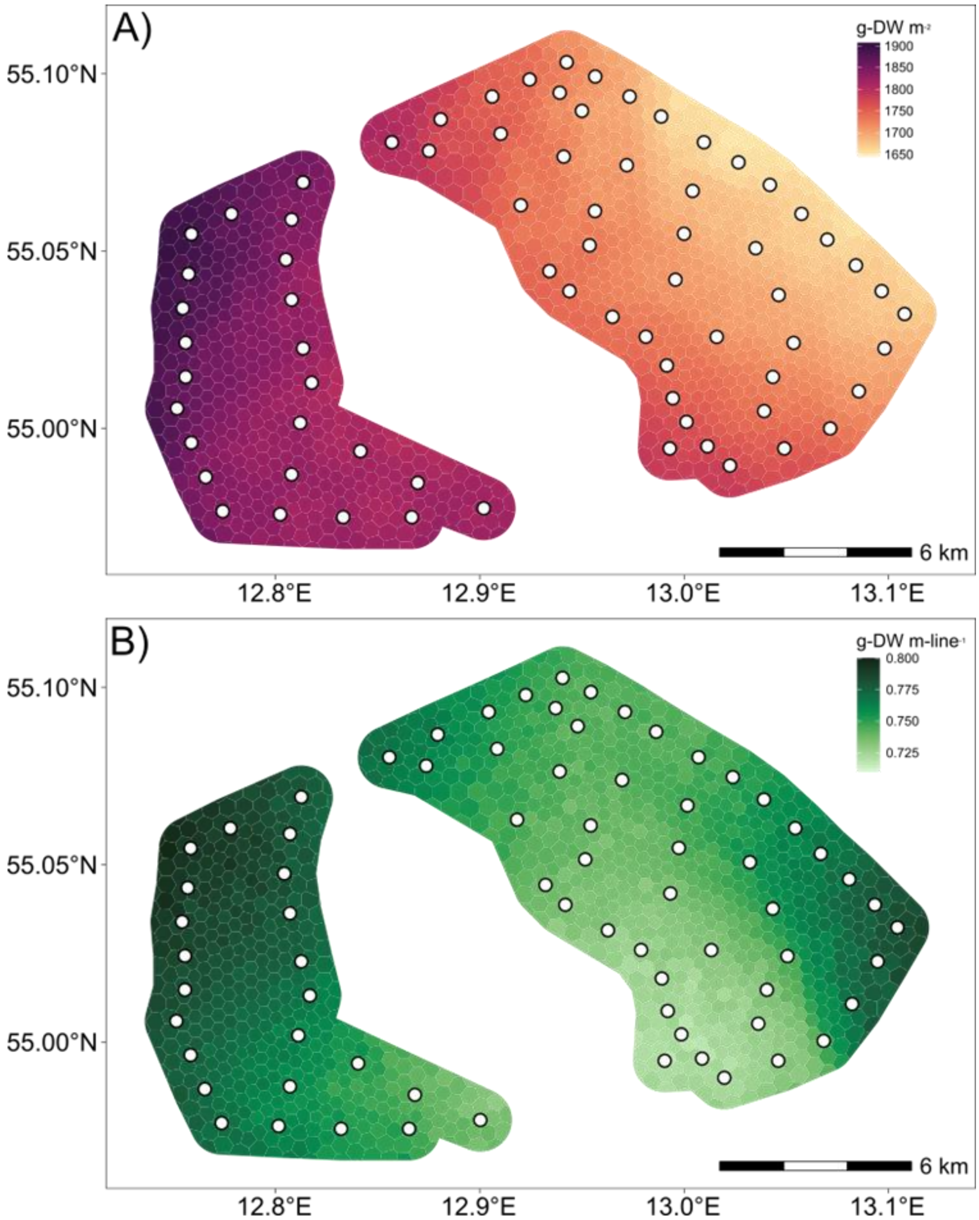

Figure 2.2.3. *Maximum potential biomass of mussel and kelp farms within the boundary of the Kriegers Flak offshore wind farm. A) Maximum potential biomass (g-DW m^{-2}) of mussels at time of harvest (31st December). B) Maximum potential biomass (g-DW m^{-2}) of kelp at time of harvest (1st June). White circles show the locations of the 72 wind turbines within the offshore wind farm.*

Based on this screening process, a harvest index (ratio from 0 to 1) was created by summing the normalised (between 0 and 1) food or nutrient flux and the normalised maximum potential biomass of mussels or kelp, respectively, and re-normalising the summed value. This provided a 'harvest potential' score for each model cell within the offshore wind farm boundary. Cells above the 66th percentile were considered as the most promising sites for aquaculture. Model cells were then divided into three categories of 'harvest potential' for co-location of mussels and kelp, dependent on the harvest potential score for each species: poor (one or both species has a score of ≤ 0.33), medium (both species have a score > 0.33, but one or both species has a score ≤ 0.66), and high (both species have a score > 0.66) (Figure 2.2.4). Areas with high

"Funded by the European Union, grant agreement NO 101094065. Views and opinions expressed are however those of the author(s) only and do not necessarily reflect those of the European Union or CINEA. Neither the European Union nor the granting authority can be held responsible for them."

‘harvest potential’ for co-location were used to inform farm placement in the different scenarios, with farms placed at increasing distance from one another. These scenarios are outlined in Table 2.2.3 and visualised in Figure 2.2.5.

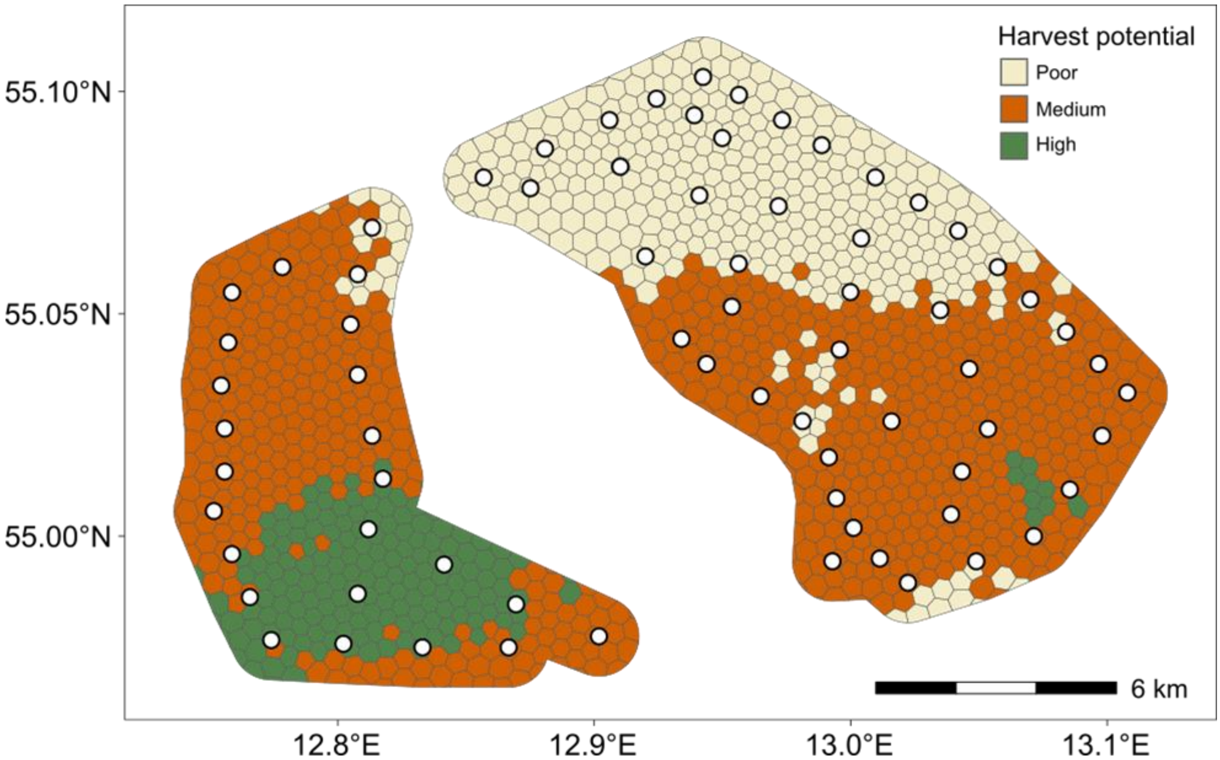

Figure 2.2.4. *Areas within the boundary of the Kriegers Flak offshore wind farm turbines with poor (yellow), medium (orange), or high (green) suitability for aquaculture of both mussels and kelp. White circles show the locations of the 72 wind turbines within the offshore wind farm.*

Table 2.2.3. *Overview of model scenarios, with mussel and kelp farms placed as increasing distance form one another.*

Scenario	Description	Number of farms	Feedback to BGM	Mussel farm	Kelp farm
M_pilot	Farm placed only in pilot farm location	1	✓	✓	×
K_pilot			✓	×	✓
M_343	Farms placed 343 m distant from one another	42	✓	✓	×
K_343			✓	×	✓
M_686	Farms placed 686 m distant from one another	22	✓	✓	×
K_686			✓	×	✓

“Funded by the European Union, grant agreement NO 101094065. Views and opinions expressed are however those of the author(s) only and do not necessarily reflect those of the European Union or CINEA. Neither the European Union nor the granting authority can be held responsible for them.”

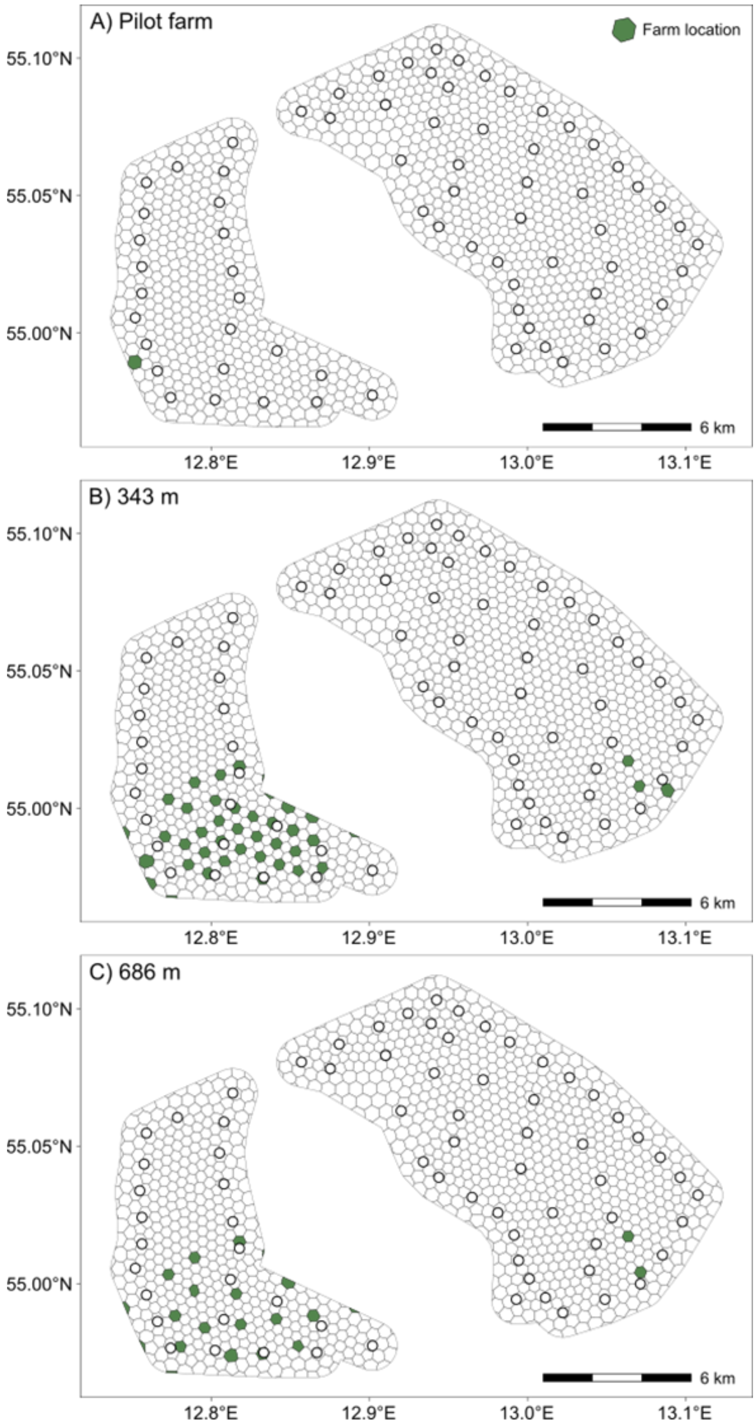

Figure 2.2.5. *Locations of mussel and kelp farms within the boundary of the Kriegers Flak offshore wind farm turbines in the different model scenarios. Green elements indicate a farm location. White circles show the locations of the 72 wind turbines within the offshore wind farm. A) Mussel and kelp farm locations for scenarios M_pilot and K_pilot. The farm is located in the model element corresponding to the location of the pilot farm at Kriegers Flak. B) Mussel and kelp farm locations for scenarios M_343 and K_343 (42 farms, 343 m distant). C) Mussel and kelp farm locations for scenarios M_686 and K_686 (22 farms, 686 m distant).*

"Funded by the European Union, grant agreement NO 101094065. Views and opinions expressed are however those of the author(s) only and do not necessarily reflect those of the European Union or CINEA. Neither the European Union nor the granting authority can be held responsible for them."

2.3. Case study C: Tagalaht Bay, Estonia

The Case Study at Tagalaht Bay in Estonia comprises a multi-use area with integrated multi-trophic aquaculture (IMTA) approach. Just within a few meters, the case study location hosts a fish farm (rainbow trout), and a multi-use plot holding a blue mussel farm and production units for seaweeds: *Ulva* and *Fucus* (Fig. 2.3.1).

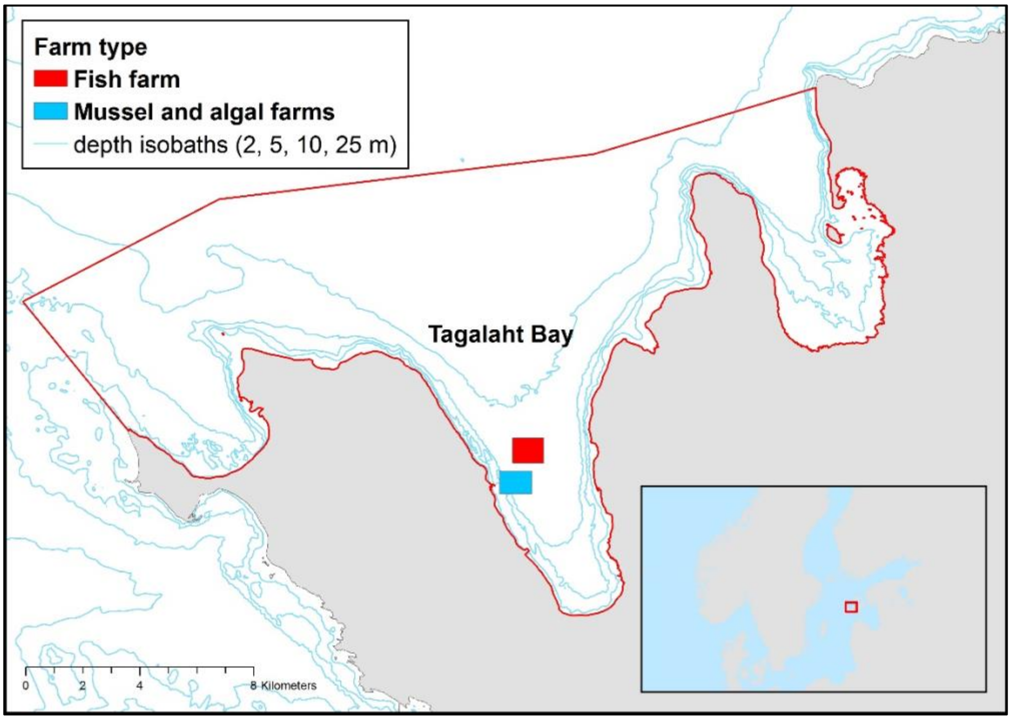

Figure 2.3.1. *Map of the Case Study area at Tagalaht Bay in Estonia.*

Rainbow Trout farm: The rainbow trout farm adjacent to the mussel farm in Tagalaht Bay consists of seven net cages, each 38 m in diameter, housing tens of thousands of fish (approx. 300 t production annually). Fish are introduced at 0.85 kg wet weight after being raised in a hatchery and are cultivated for six months (May–October). Feed is delivered via boats but cannot be distributed during storms (wave height >2 m), potentially affecting growth rates. Fish are fed with Blue Impact pellets (6 mm for smaller fish, 8 mm for larger fish), with nutrient emissions decreasing as fish grow due to the lower nitrogen (N) and phosphorus (P) content in larger pellets. Most phosphorus settles on the seabed as non-bioavailable hydroxyapatite, reducing its environmental impact.

Blue mussel farm: The test mussel farm in Tagalaht Bay (0.25 ha) uses a self-regulating system that relies on larvae recruitment from wild populations. Mussels are cultivated on nets at 1–5 m depth (SmartFarm A/S). The farm has six 100 m long lines with a stocking density of about 40 million mussels. The farm is cleaned and harvested with specialized machines after a 1.5-year cycle, from June to October of the following year.

Fucus seaweed farm: The test seaweed farm in Tagalaht Bay focuses on cultivating a local variety of *Fucus vesiculosus*, a naturally drifting form found on the seafloor, which is well-suited for cultivation in mesh cage setups. This variety is native to Estonia's coastal waters.

"Funded by the European Union, grant agreement NO 101094065. Views and opinions expressed are however those of the author(s) only and do not necessarily reflect those of the European Union or CINEA. Neither the European Union nor the granting authority can be held responsible for them."

Cultivation relies on harvested seaweed that is transported and set-up in farms where it is allowed to grow freely. The farm consists of a net cage structure floating on the surface, supported by a buoyant ring. The net is attached and kept stretched by a ballast ring, this allows *Fucus* to develop at a depth down to 1.5 meters, with an algal layer approximately 50 cm thick. Each farm unit covers an area of 6 m^2, and cultivation takes place from April to October.

2.3.1. Description of modelling approach

Tagalaht Bay is a small area, and the modelling approach in this pilot study focused specifically on the bay. For this case study, we used available data derived from large-scale ocean circulation and biogeochemical models to generate environmental conditions for the bay, including temperature, salinity, NO_3, wave conditions, current velocity, and Chl *a*. Input data were sourced from the Copernicus Marine Service, incorporating high-resolution outputs from models such as HIROMB-BOOS, BALMFC-ERGOM, and NEMO (https://data.marine.copernicus.eu/product/BALTICSEA_MULTIYEAR_PHY_003_011/services). These datasets were used to calculate nutrient and chlorophyll fluxes and used as input into the IBM-DEB models used to simulate the farms and to assess the production potential in Tagalaht bay.

Despite the relatively high resolution of these models, their application to Tagalaht Bay remains coarse (~1.5 km resolution). In this task, population models developed for rainbow trout, mussels, and seaweed were applied to the available data for Tagalaht Bay to estimate potential production under realistic farming scenarios. Single-box simulations were performed for each model cell, and all simulations for each farm/species were run independently, assuming no other activities occurred in the area.

Rainbow Trout farm: The DEB parameters used for *O. mykiss* were based on the parameter estimation published in the AmP database (2022, https://www.bio.vu.nl/thb/deb/deblab/add_my_pet/entries_web/Oncorhynchus_mykiss/Oncorhynchus_mykiss_res.html) and location-specific data from a commercial farm in Tagalaht Bay. The parameters of the temperature correction function $T_A, T_H, T_{AH}, T_L, T_{AL}$ were updated using growth data at the upper thermal tolerance of the species (Chen et al., 2015).

Zero-variate datasets included ages, DW of tissue or wet weights of tissue of all important life stages (hatch, birth, puberty) (From & Rasmussen, 1991; Davidson et al., 2014). Ultimate life span, ultimate length, ultimate wet weight, and maximum reproduction rate were also included (Tyler et al., 1996; Fishbase, 2022 http://www.fishbase.org/summary/239). Univariate datasets included hatching time at different temperatures (Velsen, 1987), growth of embryos (Ninness et al., 2006), growth of fingerlings (Yanik et al., 2002), oxygen consumption (Wieser, 1985; Lauff & Wood, 1996; Kieffer et al., 1998), and measurements of wet weight during starvation (Sumpter et al., 1991; Weatherley & Gill, 1981). To get location-relevant information, unpublished growth data was included from 4 net pens of a commercial farm in Estonia (Redstorm Ltd.). The feeding of cage 4 was lower ($f = 0.65$) than the other cages ($f = 0.7$) due to suppressed appetite (personal comment from farmer) and food availability was considered constant (Stavrakidis-Zachou et al., 2019). The temperature profile at the site was based on *in situ* measurements using a calibrated Optode-type oxygen sensor (Aanderaa

"Funded by the European Union, grant agreement NO 101094065. Views and opinions expressed are however those of the author(s) only and do not necessarily reflect those of the European Union or CINEA. Neither the European Union nor the granting authority can be held responsible for them."

Instruments) that also records temperature. Validation was done by estimating fish weights and feed efficiency ratios based on the feeding rates published by Davidson et al., (2014).

Blue mussel farm: The DEB model parameters were based on Roberts & Kooijman (2019) and were complemented with existing evidence on important life history events and metabolic characteristics. Thirteen uni- and multivariate datasets were included in the estimation process and included: total wet weight of mussels (Veber, 1998), clearance and biodeposition rates collected at different locations across the Baltic Sea (Kotta et al., 2005; Lauringson et al., 2009). Mussel growth (DW) was monitored during lab experiments at salinities of 7 and 20, an average Chl a concentration of 3.8 µg L^{-1} and a temperature of 10.8 °C (Riisgård et al., 2013). The elementary composition of the organic compounds and the shell (defined in the model as a part of structure) was defined based on measurements of N and P content in mussel tissue (Buer et al., 2020), total mussel DW (Kotta et al., 2020) and total mussel wet weight (Petersen & Loo, 2004; Buer et al., 2020).

Fucus seaweed farm: A different modelling approach was used for *Fucus*. In this case a simple, mechanistically founded model was applied. This model was derived from the *Saccharina* model used in Pilot B and follows the same set of assumptions. The *Fucus* model includes several extensions to accommodate the unique data types available and the biological differences of the species. We did not fit a salinity scaling function. Although salinity in the Baltic Sea is low, the model had already been calibrated for low salinity, and the available data did not cover a wide enough salinity gradient to justify fitting a new function (Tagalaht Bay salinity ranges from 5.5 to 6.5). However, we parameterized and calibrated scaling functions affecting the daily biomass increment to account for the effects of temperature (0 to 21 °C in Tagalaht Bay) and nitrates. The data used to calibrate the model showed that such scaling functions were needed to properly describe *Fucus* growth during the production cycle in Tagalaht Bay. In this manner, the equation in section 3.1.4 becomes:

$$\Delta M = T_f \times \left[\left(\alpha \times N_f\right) \times M_{CH_2O} \times I_{abs} - (r \times M)\right]$$

Where T_f is a scaling factor for temperature effect affecting both photosynthesis and respiration and therefore scaling growth and N_f is a scaling factor for photosynthesis to describe the limitation by the availability of NO_3 without affecting dark respiration.

The parameterization of these scaling function is as follows: for temperature, we used the Arrhenius concept as described by Kooijman et al. (2010) for Dynamic Energy Budget models to describe the effect of temperature on the growth rate of *Fucus*. We used:

$$T_f = exp\left\{\frac{T_A}{T_1} - \frac{T_A}{T}\right\} \cdot \left(1 + exp\left\{\frac{T_{AL}}{T} - \frac{T_{AL}}{T_L}\right\} + exp\left\{\frac{T_{AH}}{T_H} - \frac{T_{AH}}{T}\right\}\right)^{-1}$$

Where T_A, T_{AL}, T_{AH} are the Arrhenius temperatures at the optimal range, beyond the lower threshold and beyond the higher threshold respectively and T_L, T_H are the lower and higher temperature thresholds (see Kooijman et al. 2010).

"Funded by the European Union, grant agreement NO 101094065. Views and opinions expressed are however those of the author(s) only and do not necessarily reflect those of the European Union or CINEA. Neither the European Union nor the granting authority can be held responsible for them."

For nitrates, we modeled the limitation by nitrogen as a function of NO_3 concentration in the water (*mmol/m³*). We parameterized it as a resource functional response following a Hollings type II function.

$$N_f = \frac{[NO_3]}{[NO_3] + k_N}$$

Where k_N is the half saturation with same units as the concentration of NO_3 (mmol/m³).

Model was calibrated using datasets of *Fucus* growth under different environmental conditions with ranges of salinity, temperature, nutrients and light relevant to the Baltic Sea region. No significant effect of salinity or phosphates on growth were encountered in these datasets and therefore only nitrate, temperature and light are used as input variables for this model.

2.3.2. Model validation

Trout and blue mussel model validations were done against empirical datasets consisting of growth and other traits under contrasting environmental conditions. In total 34 and 32 datasets, for trout and mussel respectively were used for model validation. In both cases, model mean relative error (MRE) for all datasets was below 0.2 (more details in Kotta et al. 2022).

For the calibration and validation of the *Fucus* model we used data from experimental farming. In late 2023, AquaVerde Ltd established the first offshore seaweed farm in the low-salinity region of the Baltic Sea at the multiuse pilot C. Initial trials were conducted as part of the HORIZON project AlgaeProBanos, examining how different farm configurations and dimensions influenced both farm stability and seaweed growth. Based on these findings, an optimal setup was chosen, and from April to October 2024, the test farm successfully cultivated the drifting form of *Fucus vesiculosus*. Data on daily growth, biomass and photosynthesis along with key environmental parameters, including water temperature, light intensity, water velocity, turbidity, salinity, and wave dynamics, were monitored using underwater autonomous instruments throughout production.

2.3.3. Run scenarios

We run realistic farm settings for rainbow trout, blue mussels and *Fucus* seaweed. The scenario runs are the set-ups used by the activity at the study case in Tagalaht Bay (Figure 4.3.1, orange dot in maps).

Aquaculture is increasingly regarded as a promising solution for meeting the growing global demand for fish, but this potential can only be realized if the industry reduces its reliance on wild-caught fish in feeds and mitigates its environmental impacts. Integrated multi-trophic aquaculture (IMTA), the practice of cultivating extractive species like macroalgae and bivalves alongside finfish, offers a potential pathway for improving environmental sustainability. By actively up-taking and assimilating dissolved nutrients released from finfish farms, these low-trophic-level organisms help remove excess nutrients from the ecosystem once they are harvested.

"Funded by the European Union, grant agreement NO 101094065. Views and opinions expressed are however those of the author(s) only and do not necessarily reflect those of the European Union or CINEA. Neither the European Union nor the granting authority can be held responsible for them."

This case study investigated the potential of mussels and macroalgae to serve as a bioremediation tool at finfish farms in the eutrophic Baltic Sea region. We run Dynamic Energy Budget (DEB) models for blue mussels (*Mytilus edulis/trossulus*) and rainbow trout (*Oncorhynchus mykiss*) and a mechanistic dynamic model for *Fucus vesiculosus* with a regional hydrodynamic-biogeochemical model to assess how mussel and macroalgae farming could compensate for nutrient discharges from finfish farms and what is the potential yield of both species in the area.

The aim of this pilot case was to analyse the potential use of blue mussels and macroalgae to mitigate the negative environmental impacts of fish farming, as discussed in Kotta et al. (2023). These scenarios do not simulate an IMTA set-up where interactions between the different farming activities and the environment are fully coupled. In this study case the run scenarios simulated the potential of each farm activity individually in the region with the aim to assess the production potential of each species and the fluxes for nutrients.

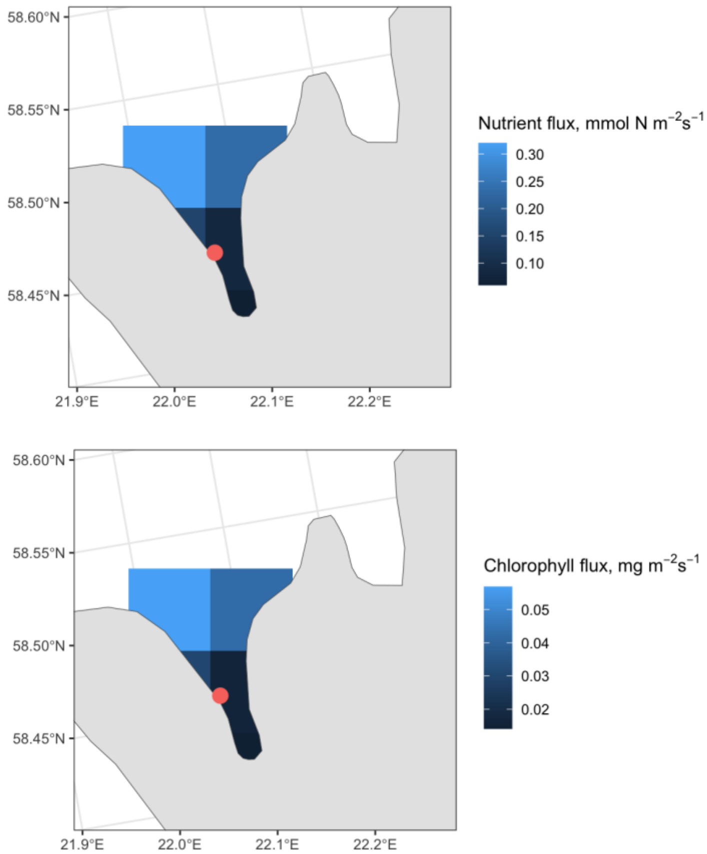

Figure 4.3.1. *Annual mean food and nutrient flux within the Tagalaht Bay. Top: Average nutrient flux (mmol* NO_3 m^{-2} s^{-1}*). Bottom: Average food flux (mg Chl* a m^{-2} s^{-1}*). Orange dot is the location of the multiuse study area (pilot C).*

"Funded by the European Union, grant agreement NO 101094065. Views and opinions expressed are however those of the author(s) only and do not necessarily reflect those of the European Union or CINEA. Neither the European Union nor the granting authority can be held responsible for them."

3. Results & discussion

3.1. Case A

3.1.1. Model Validation results

The model simulation accurately reflects the development and magnitude of the average chlorophyll-a concentration. It was found that there was a slight deviation in the timing of the spring bloom, which began slightly earlier than expected (Fig. 3.1.1). Additionally, the simulated chlorophyll-a concentrations in autumn were found to be relatively low. The model's representation of the spatial distribution of the spring bloom was satisfactory, with only minor deviations observed in the coastal area (Fig. 3.1.2).

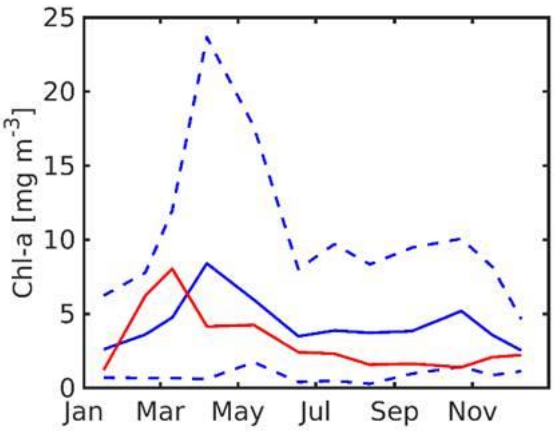

Figure 3.1.1. *Mean surface chlorophyll-a given by in-situ observations in the model area of the southern North Sea (blue solid line) with 5th and 95th percentiles of represented by the blue dashed lines. The red solid line shows the simulated monthly dynamics averaging over the model nodes closest to the respective in-situ observations.*

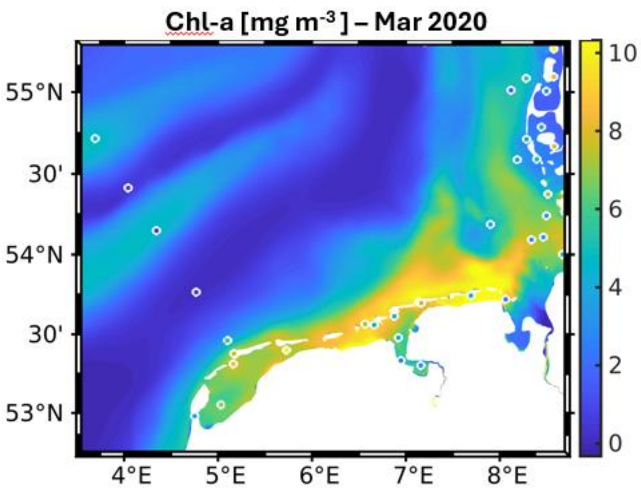

Figure 3.1.2. *Observations of surface chlorophyll-a during March 2020 provided via the ICES website (circs) against the background of simulated monthly mean chlorophyll-a in the area of the German Bight and Dutch Wadden Sea of the southern North Sea.*

Validation of blue mussel growth

"Funded by the European Union, grant agreement NO 101094065. Views and opinions expressed are however those of the author(s) only and do not necessarily reflect those of the European Union or CINEA. Neither the European Union nor the granting authority can be held responsible for them."

Within the reporting period blue mussel samples have been taken from the marker buoys surrounding the Smart Farm operated by WP1. The mussel samples were taken from different buoys in May and August, most likely representing individuals in the second year of life. Figure 3.1.3 shows the weight distributions found at the sampling sites. The median mussel dry weight increased from 1.96 g ind^{-1} to 2.63 g ind^{-1} between the first and second round of sampling resulting in median increase of 0.67 g ind^{-1}. A simulation of blue mussel dynamics at the Smart Farm location resulted in median dry weight increase of 1.63 g ind^{-1} taking into account May to August from the first and the second year following initialisation. For a better comparability of in-situ and simulated data it is necessary to obtain blue mussel growth from consistently initialised individuals. However, the difficulties to take the pilot A into production has limited the availability of in-situ samples from the farming structures.

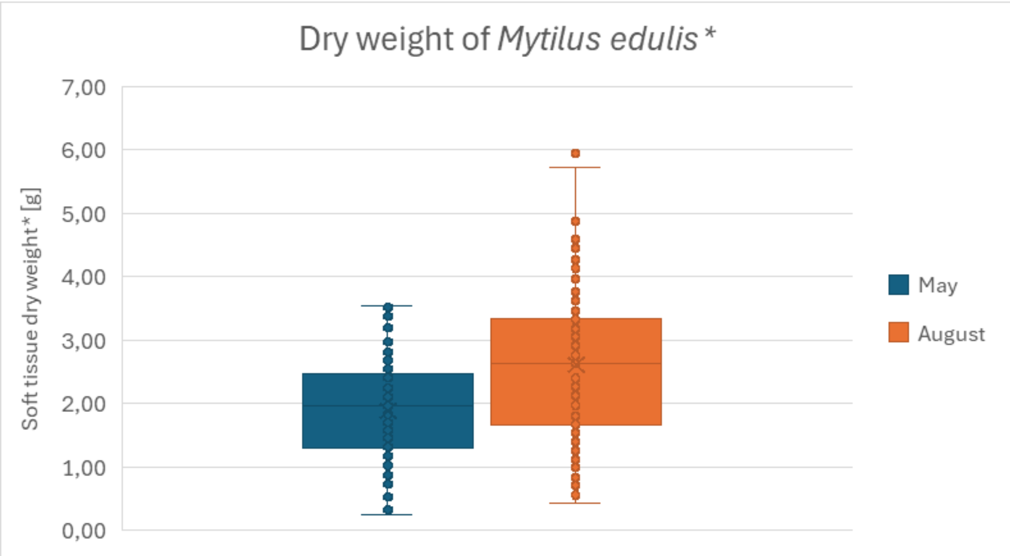

Figure 3.1.3. *Dry weight of blue mussels sampled at the marker buoys in the area of the Meerwind windfarm (Data: Zambalos/Wolf/Buck - AWI) in May and September 2025, whereas the dry weight has been estimated from total weight (Larsen et al., 2013). In these box plots the thin grey line within the colored rectangles refers to the statistical median.*

3.1.2. Growth/Productivity results (scenarios)

The scenario set-up has been described in Section 2.1.3. In the screening scenario ("M0") highest potential farm biomass occurred in the western and central part of the windfarm polygon (Fig. 3.1.4), whereas the mean harvest potential was 19.1 kg-DW m^{-2}. In general, the potential was higher close to the windfarm monopiles then in between them.

"Funded by the European Union, grant agreement NO 101094065. Views and opinions expressed are however those of the author(s) only and do not necessarily reflect those of the European Union or CINEA. Neither the European Union nor the granting authority can be held responsible for them."

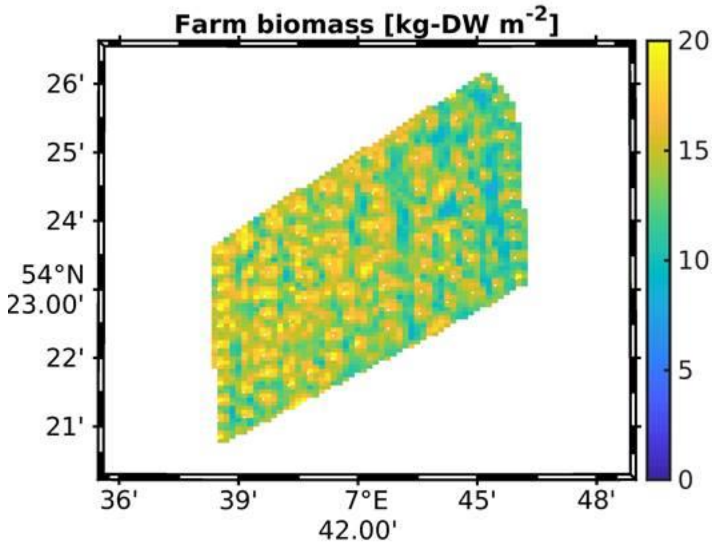

Figure 3.1.4. *Screening scenario ("M0") with the farm biomass of blue mussel aquaculture. The white dots indicate position of windfarm monopiles.*

In the realistic blue mussel farming scenarios, the highest estimated farm biomass is achieved in the minimal and reference scenario "M1" implementing a small farm array of 2.2 ha size in the south-eastern part of the windfarm (Fig. 3.1.5a). Here, the farm biomass achieved about 5.3 kg-DW m^{-2}.

In the second scenario, "M2" the farm biomass achieved was generally lower with 3.2 kg-DW on average (Fig 3.1.5b). In the location of the farm in "M1", "M2" farms revealed considerably lower yield of about 3.6 kg-DW m^{-2}. However higher yields were achieved in the western and central part of the windfarm confirming the initial assessment provided by the screening scenario ("M0", Fig. 3.1.4). Increasing the distance between farms from 350 m in "M2" to 700 m in "M3" led to estimated harvest potential of 3.7 kg-DW m^{-2} at the end of the season.

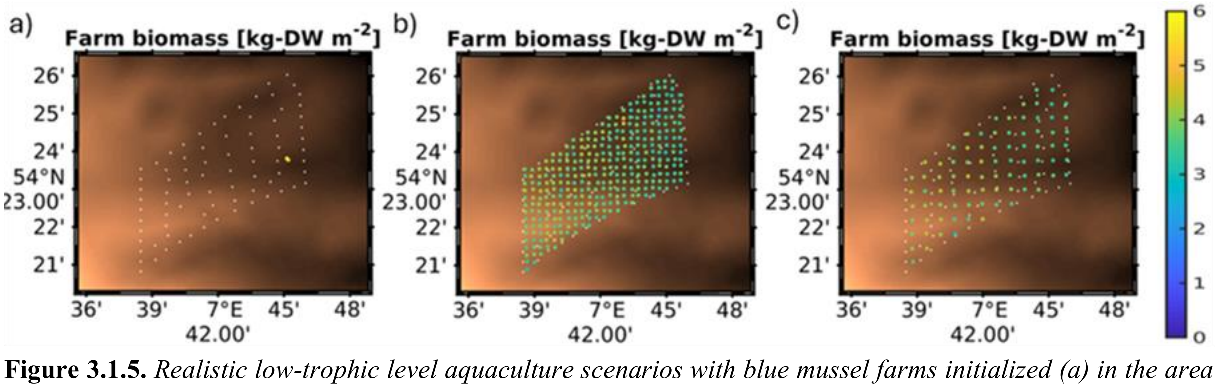

Figure 3.1.5. *Realistic low-trophic level aquaculture scenarios with blue mussel farms initialized (a) in the area of the experimental farm of WP1 case study A ("M1"), (b) equally spaced in the area of the windfarm with a nominal distance of 350 m ("M2"), (c) equally spaced in the area of the windfarm with a nominal distance of 700 m ("M3").*

These results indicate that increasing the number of farms with the windpark leads to reduced yield of the individual farm and that the exact siting of aquaculture farms can be optimized.

"Funded by the European Union, grant agreement NO 101094065. Views and opinions expressed are however those of the author(s) only and do not necessarily reflect those of the European Union or CINEA. Neither the European Union nor the granting authority can be held responsible for them."

3.1.3. Ecosystem services results.

While aquaculture directly reduces phytoplankton levels by removing them from the system, it can indirectly have the opposite effect due to the complex interactions between currents, nutrient supply, primary production and zooplankton grazing. In this case, the most realistic scenario involving a single aquaculture farm (“M1”) resulted in an increased local chlorophyll a concentration of 2.3 mg m^{-3} in the area of the wind farm, which was only slightly less than the concentration of 2 mg m^{-3} in the immediate vicinity (Fig. 3.1.6a). As expected, the “M2” scenario, involving several aquaculture farms spaced 350 metres apart across the wind farm, resulted in a phytoplankton concentration reduction of approximately 1e-3 mg m^{-3} during the comparison period (Fig. 3.1.6b). By contrast, the "M3" scenario, with aquaculture farms spaced 750 m apart, led to an increase in phytoplankton concentration in the wind farm and its northern surroundings (Fig. 3.1.6c). This result indicates that, under certain conditions, the removal of phytoplankton can stimulate its growth, creating a positive feedback loop. In this case, the ecosystem service of reducing chlorophyll is not optimally realised.

Similar to chlorophyll, dissolved phosphate also showed a local maximum in the area of the wind farm, with values slightly above zero (generally very low) reaching 0.03 mmol m^{-3} (see Fig. 3.1.6d and a recent report on dissolved inorganic phosphorus as a limiting factor for phytoplankton growth in the North Sea: Duteil et al., 2023). Compared to scenario “M1”, scenario 'M2' showed a slight reduction in the north and a slight increase in the south of the wind farm in terms of phosphate (see Fig. 3.1.6e). In contrast, scenario “M3” showed a relatively significant reduction in phosphate of up to 0.05 mmol m^{-3} in the central and southern parts of the area compared to the “M1” reference scenario (Fig. 3.1.6f), which is consistent with the increased phytoplankton concentration in this scenario and time period.

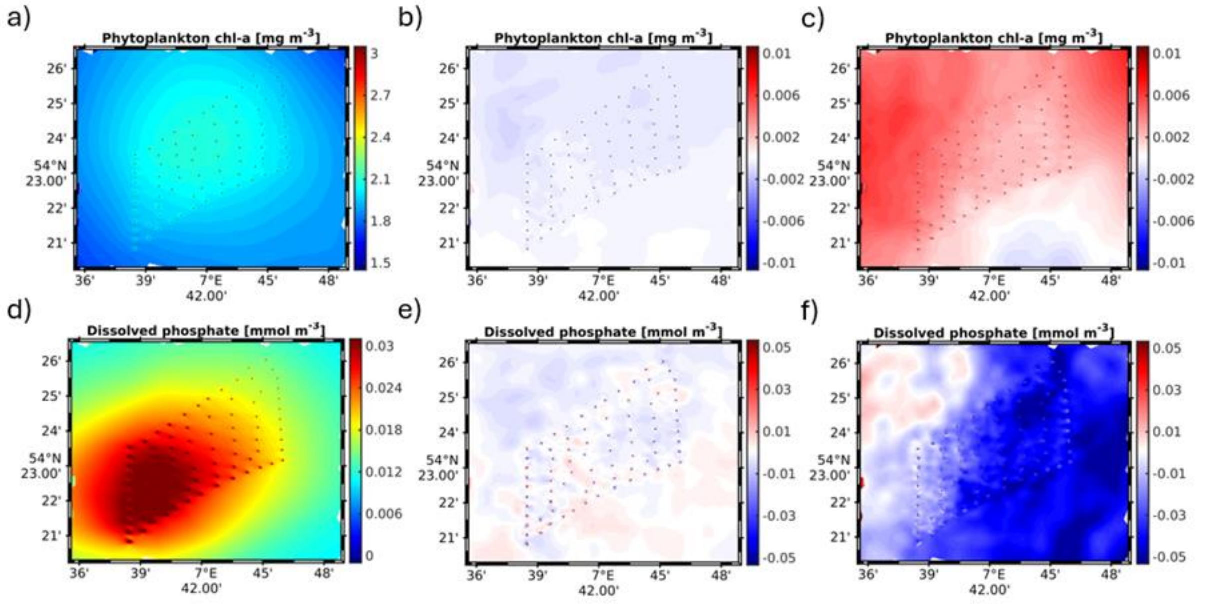

Figure 3.1.6. *Surface concentrations of (a) chlorophyll-a and (d) dissolved phosphate in the reference aquaculture farm scenario (“M1”) during May-September 2020 with (b,c) and (e,f) showing the difference plots scenario minus reference for “M2” and “M3” scenarios, respectively.*

“Funded by the European Union, grant agreement NO 101094065. Views and opinions expressed are however those of the author(s) only and do not necessarily reflect those of the European Union or CINEA. Neither the European Union nor the granting authority can be held responsible for them.”

The distribution of dissolved inorganic nitrogen differs from previous nutrients showing primarily zonal variability (Fig. 3.1.7a). The differences between “M2” and “M1” scenarios appear to be negligeable, whereas “M3” demonstrates consistent reduction of dissolved inorganic nitrogen in comparison with “M1” scenario (Fig. 3.1.7b, c).

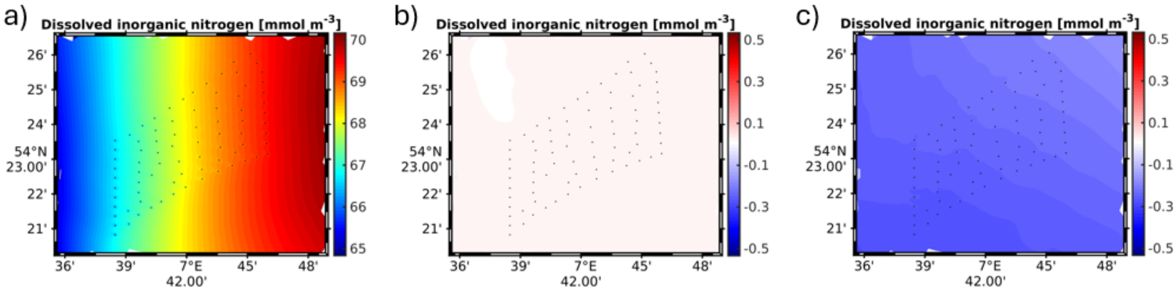

Figure 3.1.7. *Surface concentrations of (a) dissolved inorganic nitrogen in the reference aquaculture farm scenario (“M1”) during May-September 2020 with (b) and (c) showing the difference plots scenario minus reference for “M2” and “M3” scenarios, respectively.*

In the reference scenario “M1”, the distribution of phytodetritus essentially followed that of chlorophyll, reaching 19 mg C m^{-3} locally (Fig. 3.1.8a). In scenarios “M2” and “M3”, there was a slight to significant reduction (see Fig. 3.1.8b and c). This highlights the absence of a reduction in chlorophyll or phytoplankton, given that the reduction in dead organic material (i.e. phytodetritus) suggests a reduction in the effects of eutrophication and a decrease in turbidity. It is possible that the reduction in phytodetritus explains the increased phytoplankton abundance, which may be due to improved light conditions or better nutrient availability.

Dissolved oxygen also exhibited a local maximum of 269 mmol O_2 m^{-3} in the vicinity of the wind farm in the reference scenario “M1”, peaking at the north-western corner of the turbine array (Fig. 3.1.8d). In scenario “M2”, the oxygen concentration increased slightly, whereas in “M2”, the increase was more systematic, amounting to approximately 0.25 mmol/m^3 (see Fig. 3.1.8 and f). In this case, placing the farms at a greater distance proved an effective strategy for improving local oxygen conditions.

“Funded by the European Union, grant agreement NO 101094065. Views and opinions expressed are however those of the author(s) only and do not necessarily reflect those of the European Union or CINEA. Neither the European Union nor the granting authority can be held responsible for them.”

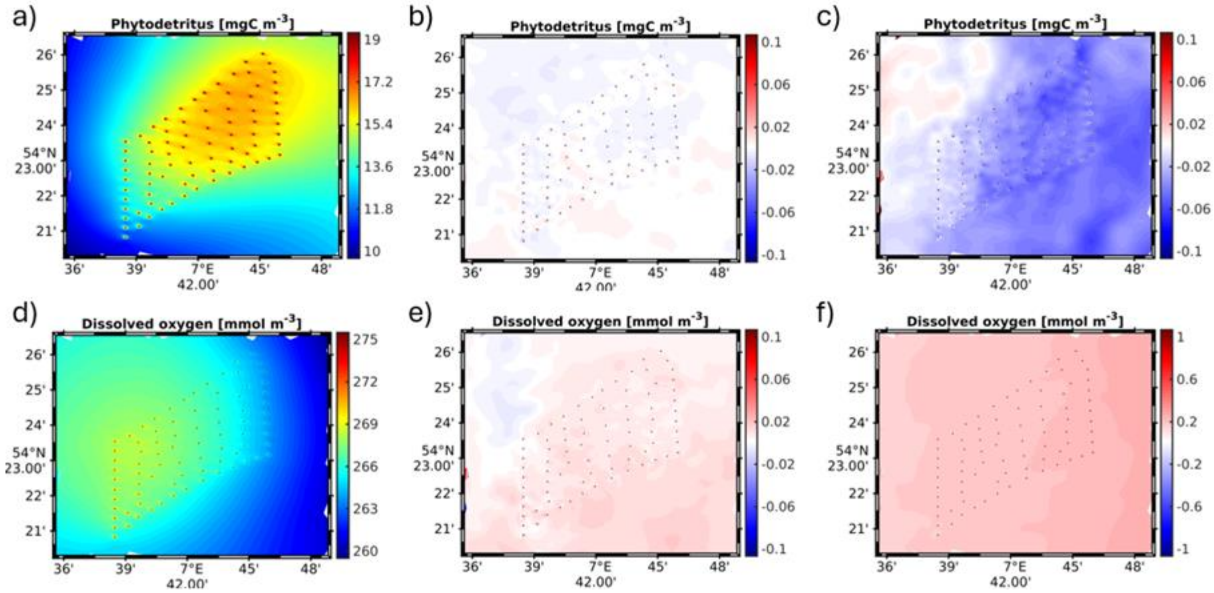

Figure 3.1.8. *Surface concentrations of (a) phyto-detritus and (d) dissolved oxygen in the minimal aquaculture farm scenario ("M1") during May-September 2020 with (b,c) and (e,f) showing the difference plots scenario minus reference for "M2" and "M3" scenarios, respectively.*

Overall, results support the hypothesis that low-trophic-level aquaculture can provide ecosystem services in terms of reduction of turbidity-drivers such as phytodetritus or increase of the oxygen concentrations. The vigorous physical environment with strong tidal currents and intense vertical mixing, further enhanced by the impact of offshore windfarm structures, favors quick spreading of biogeochemical/biological effects at least on the farm-scale. Physics clearly dominate the spatial patterns where the local mixing by the windfarm monopiles was mostly well visible (e.g. surface dissolved oxygen, Fig. 3.1.6d). Aquaculture impacts on the other hand cannot be visibly tracked to the single farms and effects appear to be smoothed and shifted in space. The results from the scenarios "M1" - "M3" are reported in table 5.1.

To fill in Table 5.1, the outputs from the biogeochemical module were combined with outputs from the physical core during post-processing. Fig. 3.1.8 illustrates the derived nutrient flux of chlorophyll-A during the summer season in the area of the *Meerwind* wind farm.

"Funded by the European Union, grant agreement NO 101094065. Views and opinions expressed are however those of the author(s) only and do not necessarily reflect those of the European Union or CINEA. Neither the European Union nor the granting authority can be held responsible for them."

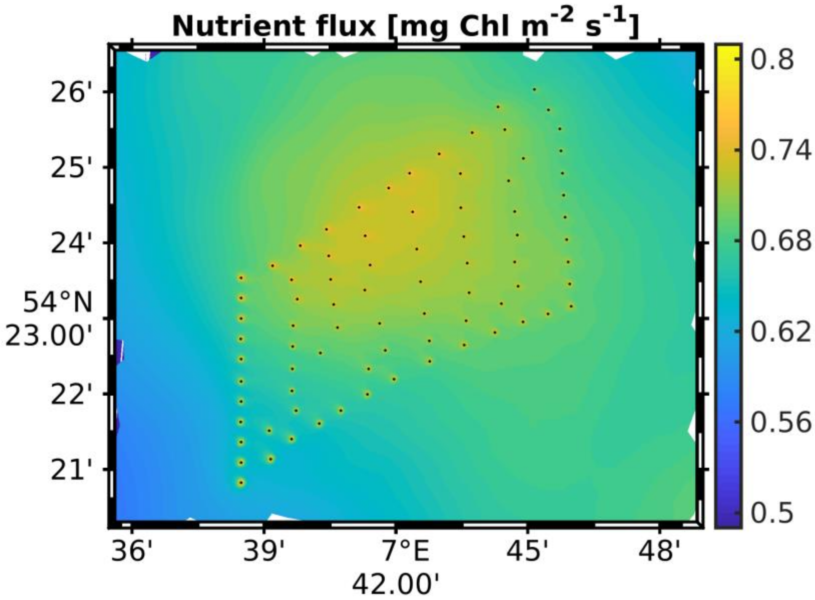

Figure 3.1.8. *Time-averaged simulated surface Chl a flux compiled from the coupled physical-biogeochemical model run during May to September 2020.*

3.2. Case B

3.2.1. Model Validation results

Environmental parameters validation

Model performance for ecological variables was all either 'good' ($CF < 1$) or 'reasonable' ($1 \leq CF \leq 2$) with the exception of bottom oxygen concentration, for which there was a 'poor' ($CF > 2$) fit and a low correlation with observations (Figure 3.2.1H; Table 3.2.1). This is likely due to too much mixing at the bottom layer in Spring. Surface values for temperature, nitrate, phosphate and oxygen showed the best agreement with observations across the calculated metrics (Figure 3.2.1A, C, D, G; Table 3.2.1). Model performance for Chl *a* and Secchi depth was both 'good', but model data did not significantly correlate with observations and both parameters were underestimated in winter months (Figure 3.2.1E, F; Table 3.2.1).

Table 3.2.1. Validation results of environmental parameters in Kriegers Flak. The results of Pearson's correlation tests (*r*), calculation of cost function *CF*), and normalised standard deviation (nSD) between parameters from the FlexSem model for Kriegers Flak and *in situ* observations from monitoring station DMU444.

Parameter	t-value	DoF	p-value	*r*	R^2	CF	nSD
Surface temperature	11.56	20	2.63×10^{-10}	0.93	0.87	0.06	1.34
Surface salinity	2.60	20	0.017	0.50	0.25	1.04	2.97
NO_3	3.11	18	0.006	0.59	0.35	0.55	0.57
PO_4	5.66	18	2.28×10^{-5}	0.80	0.64	0.47	1.09
Chl *a*	1.28	18	0.217	0.29	0.08	0.11	2.01
Secchi depth	0.96	13	0.353	0.26	0.07	0.03	1.36

"Funded by the European Union, grant agreement NO 101094065. Views and opinions expressed are however those of the author(s) only and do not necessarily reflect those of the European Union or CINEA. Neither the European Union nor the granting authority can be held responsible for them."

Surface O_2	7.48	21	2.38×10^{-7}	0.85	0.73	0.18	1.30
Bottom O_2	-1.63	5	0.163	-0.59	0.35	2.36	1.56

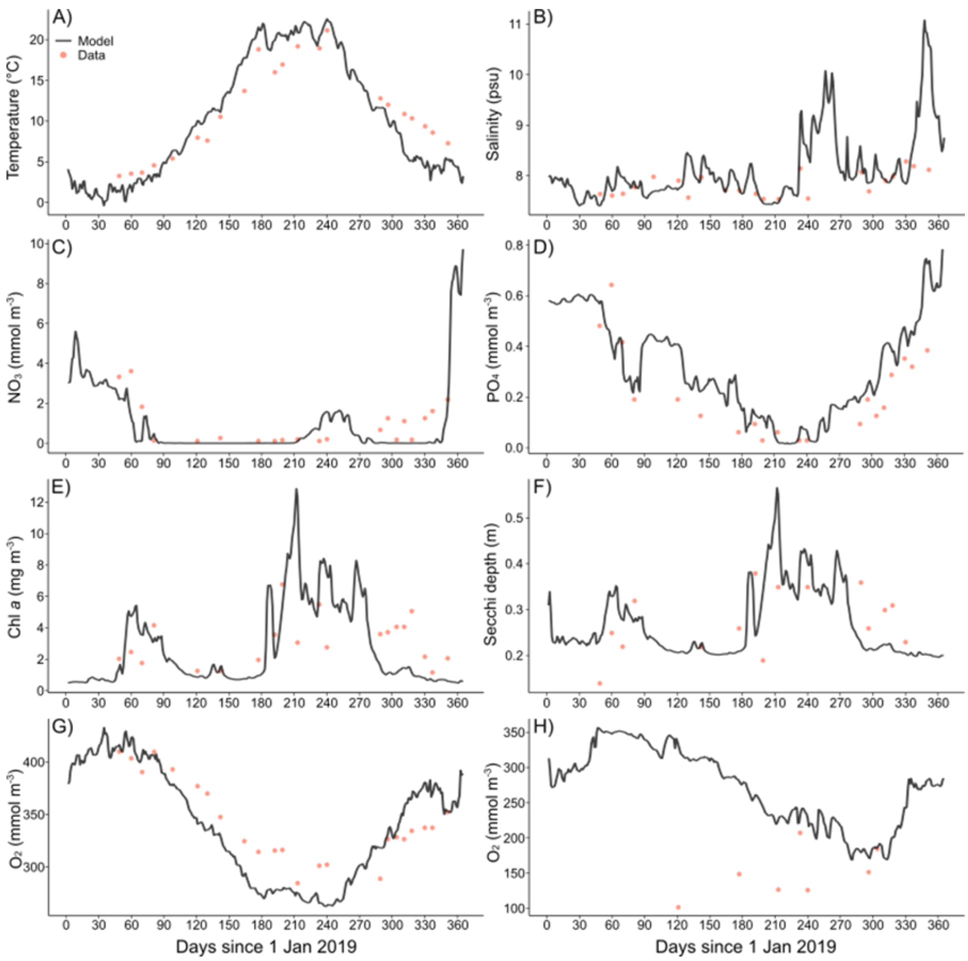

Figure 3.2.1. *Model calibration of water column properties at the monitoring station DMU444. A) Surface temperature (°C); B) Surface salinity (psu); C) Surface nitrate concentrations (mmol m^{-3}); D) Surface phosphate concentrations (mmol m^{-3}); E) Surface chlorophyll a concentration (mg m^{-3}); F) Secchi depth (m); G) Surface oxygen concentration (mmol m^{-3}); and H) Bottom oxygen concentration (mmol m^{-3}). Lines show the model output, whilst points show the observations from DMU444.*

Mussel model validation

The model was calibrated using measurements of mussels deployed using the New Zealand collector type and showed overall the best fit to those data compared to the Bendler collector type. However, data for these New Zealand collectors was only available for one point in time as the mussel farmer was unable to maintain the lines. The New Zealand collector type had a four times higher mussel density than the Bendler type. Hence, some deviation between the mussel model and Bendler data was expected. Model results for mussel biomass (kg-DW m^{-1}) at 3 m depth showed some agreement with measurements of the mussels at the pilot farm (Figure 3.2.2A). The model shows strong agreement with the measurement from New Zealand collectors, and with a measurement from the mussels grown using the Bendler collector type taken in June, but overestimates biomass of mussels grown using the Bendler collection type early in the year (Figure 3.2.2A). Equally, the model results for mussel density (ind. m^{-1}) and

"Funded by the European Union, grant agreement NO 101094065. Views and opinions expressed are however those of the author(s) only and do not necessarily reflect those of the European Union or CINEA. Neither the European Union nor the granting authority can be held responsible for them."

individual dry weight (g) show strong agreement with the measurement of the New Zealand collector mussels (Figure 3.2.2B, C). In the case of density, the model somewhat overestimated the density of mussels grown on the Bendler collector type (Figure 3.2.2B), however model values for individual dry weight were within the standard deviations of the Bendler observations (Figure 3.2.2C). Model results for mussel shell length (cm) showed a strong agreement with measurements of mussels from both the New Zealand and Bendler collector types (Figure 3.2.2D).

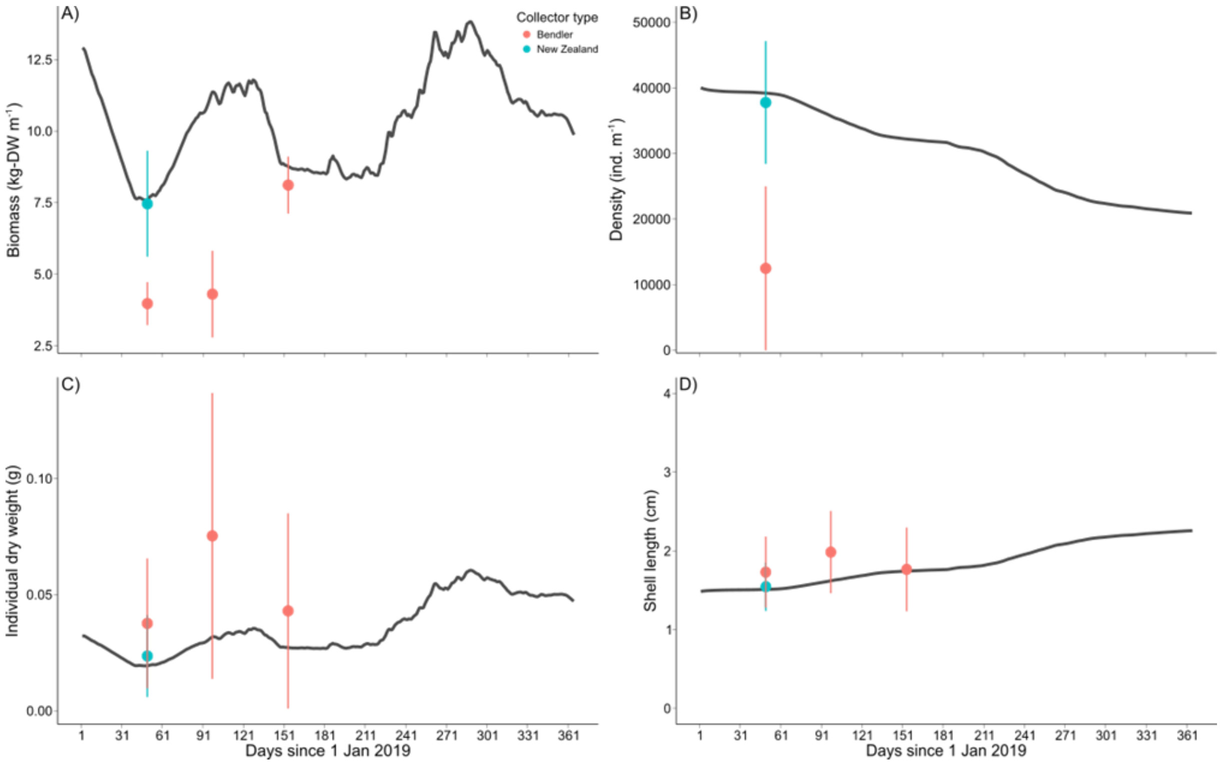

Figure 3.2.2. *Model calibration of Mytilus sp. biomass (kg-DW m $^{-1}$), density (ind. m $^{-1}$), individual dry weight (g) and shell length (cm) with measurements from the pilot farm at Kriegers Flak. Solid line shows the results of the model when no feedback to the biogeochemical model was included. Points show the average (± SD) of measurements taken from the pilot farm for two mussel collector types (colour). Data cover the period 1 Jan 2019 – 31 Dec 2019 and are from 3 m depth. A) Mussel biomass; B) mussel density; C) mussel individual dry weight; D) mussel shell length. The model was calibrated against the New Zealand bendler.*

The model somewhat overestimated mussel nitrogen content (g-N g-DW $^{-1}$) compared to measurements taken from the pilot farm in April but was a good fit to measurements taken in June (Figure 3.2.3A). The model somewhat overestimated mussel carbon content (g-C g-DW $^{-1}$) compared to measurements taken from the pilot farms but was within a range of ~0.2 from observations (Figure 2.2.3B).

"Funded by the European Union, grant agreement NO 101094065. Views and opinions expressed are however those of the author(s) only and do not necessarily reflect those of the European Union or CINEA. Neither the European Union nor the granting authority can be held responsible for them."

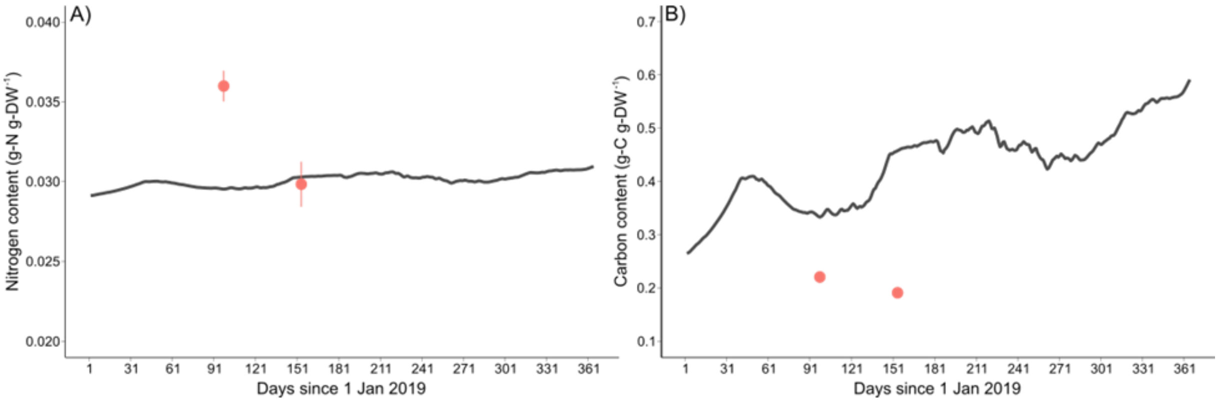

Figure 3.2.3. *Model calibration of Mytilus sp. nitrogen content (g-N g-DW^{-1}) and shell carbon content (g-C g-DW^{-1}) with measurements from the pilot farm at Kriegers Flak. Solid line shows the results of the model when no feedback to the biogeochemical model was included. Points show the average (± SD) of measurements taken from the pilot farm. Data cover the period 1 Jan 2019 – 31 Dec 2019 and are from 3 m depth. A) Whole mussel nitrogen content; B) mussel shell carbon content.*

Kelp model validation

Model results for kelp biomass (g-DW m-line^{-1}) at 1 m depth showed a strong agreement with measurements from the kelp deployed in 2024 (Figure 3.2.4A). At 3 m and 6 m depth there was strong agreement with measurements of kelp biomass from the Middelfart strain deployed in 2023, with model results falling within the standard deviation from the average biomass value for both salinity adapted and non-salinity adapted kelp (Figure 3.2.4B, C). Although the Kiel strain of kelp produced greater biomass than the Middelfart strain, we calibrated our model towards the Middelfart values as there were no data from the Kiel strain for 2024.

As for biomass, model results for frond length (m) at 1 m depth showed a strong agreement with measurements from the kelp deployed in 2024, but equally model results were not too dissimilar from measurements of the Kiel strain of kelp deployed in 2023 (Figure 3.2.4D). Measurements from the Middelfart strain deployed in 2023 were much lower, likely because in 2023 lines were deployed later in autumn (non-optimal) than for the 2024 deployment. Hence, the Middelfart data from 2023 was assumed not to be representative for the area.

"Funded by the European Union, grant agreement NO 101094065. Views and opinions expressed are however those of the author(s) only and do not necessarily reflect those of the European Union or CINEA. Neither the European Union nor the granting authority can be held responsible for them."

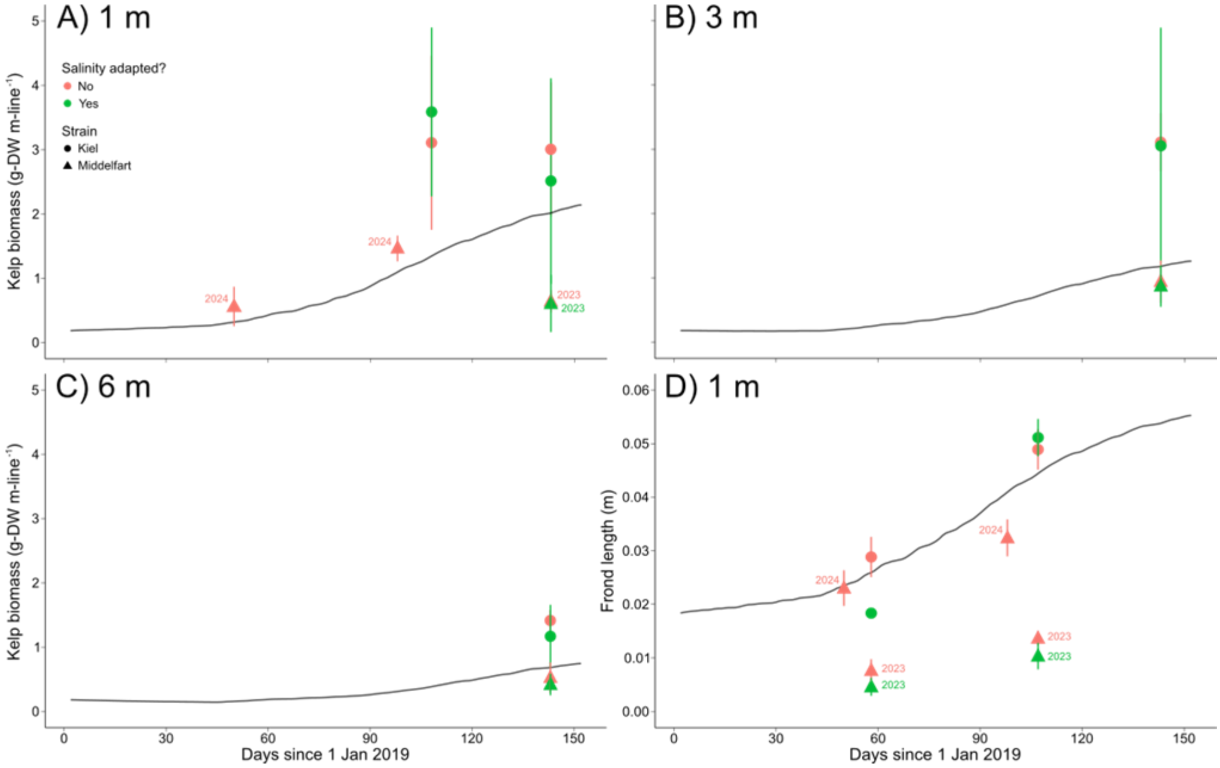

Figure 3.2.4. *Model calibration of Saccharina latissima biomass (g-DW m-line^{-1}) and frond length (m) with measurements from the pilot farm at Kriegers Flak. Solid line shows the results of the model when no feedback to the biogeochemical model was included. Points show the average (± SD) of measurements taken from the pilot farm for two strains of kelp (colour) that had either had or had not undergone salinity adaptation (shape) and were deployed in either 2023 or 2024 (labelled). Data covers the period 1 Jan 2019 – 1 Jun 2019 (day 152) – the production period for S. latissima biomass. A) Kelp biomass at 1 m depth; B) kelp biomass at 3 m depth; C) kelp biomass at 6 m depth; D) kelp frond length at 1 m depth.*

Finally, model results for nitrogen content of kelp (g-N g-DW^{-1}) at 1 m depth showed a strong agreement with measurements from the pilot farm, falling within the standard deviations of the average values (Figure 3.2.5).

"Funded by the European Union, grant agreement NO 101094065. Views and opinions expressed are however those of the author(s) only and do not necessarily reflect those of the European Union or CINEA. Neither the European Union nor the granting authority can be held responsible for them."

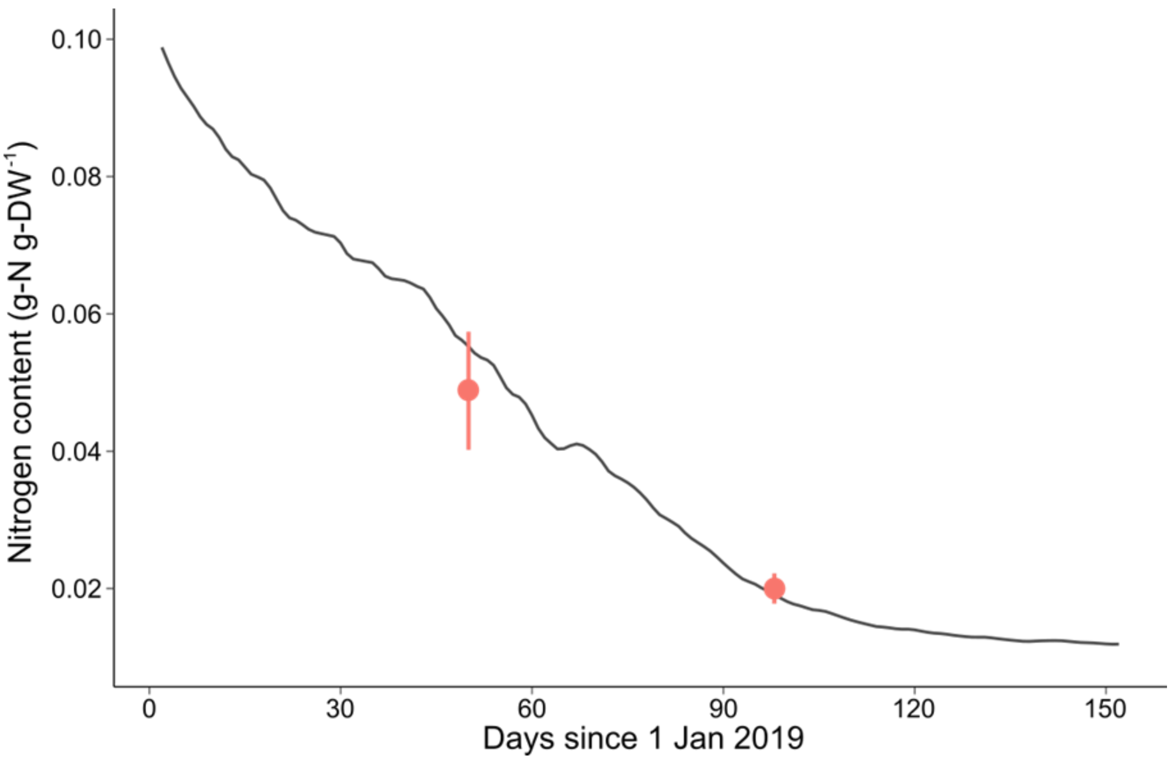

Figure 3.2.5. *Model calibration of Saccharina latissima nitrogen content (g-N g-DW^{-1}) with measurements from the pilot farm at Kriegers Flak. Solid line shows the results of the model when no feedback to the biogeochemical model was included. Points show the average (± SD) of measurements taken from the pilot farm. Data cover the period 1 Jan 2019 – 1 Jun 2019 (day 152) – the production period for S. latissima biomass.*

3.2.2. Growth/Productivity results

Mussel biomass and shell length

At the time of harvest (31st December) mussel biomass from 2 – 5 m depth at the pilot farm location (M_pilot) was 810.54 g-DW m^{-2}, and the average shell length was 2.37 cm (Figure 3.2.6). Mussel biomass per individual farm at the time of harvest was greater in scenario M_686, where farms were placed 686 m distant from one another, than scenario M_343, where they were placed 343 m distant (Figure 3.2.6). The same pattern was evident for the average shell length of individuals (Figure 3.2.6). This would suggest that when placed too closely together adjacent mussel farms negatively impact one another through depletion of food and nutrients, leading to reduction in growth. This is supported by the fact that the biomass in scenarios M_343 and M_686 is lower than for the M_pilot scenario, where only one farm was modelled.

"Funded by the European Union, grant agreement NO 101094065. Views and opinions expressed are however those of the author(s) only and do not necessarily reflect those of the European Union or CINEA. Neither the European Union nor the granting authority can be held responsible for them."

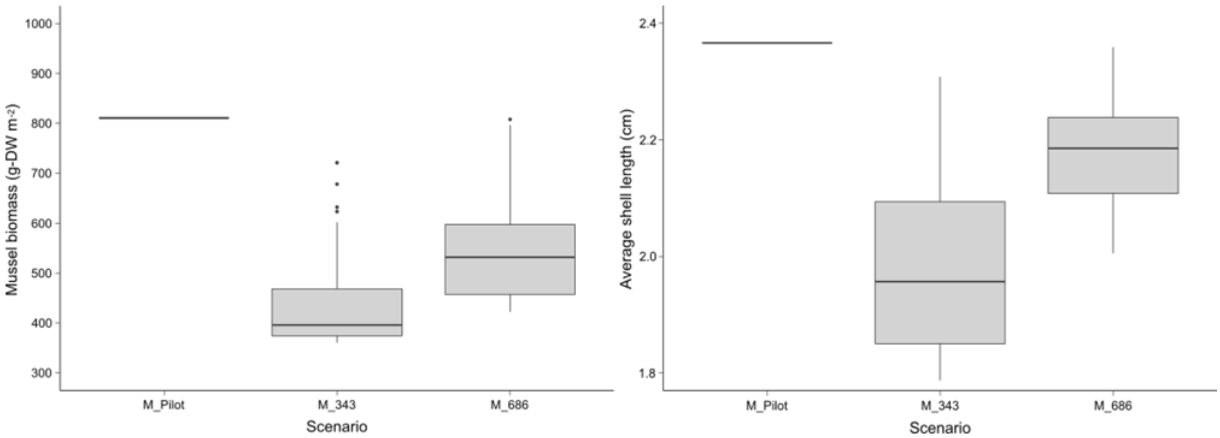

Figure 3.2.6. *(Left) Total mussel biomass (g-DW m^{-2}), and (Right) average shell length of individuals (cm) for each farm at time of harvest (31st December) for scenarios M_pilot (single farm in pilot location), M_343 (42 farms placed 343 m distant from one another) and M_686 (22 farms placed 686 m distant from one another).*

Kelp biomass

At the time of harvest (1st June) kelp biomass from 0 – 6 m depth at the pilot farm location (K_pilot) was 0.87 g-DW m^{-2} (Figure 3.2.7). The median value for kelp biomass per individual farm at time of harvest was marginally greater in scenario K_686, where farms were placed 686 m distant from one another, than scenario K_343, where they were placed 343 m distant (Figure 3.2.7). This would suggest that when placed too closely together there is an effect of nitrogen depletion on kelp growth, leading to reduced biomass. However, the small scale of the differences in biomass between the K_343 and K_686 scenarios (~0.01 g-DW m^{-2}) would suggest that this effect is minor. This is likely due to the very minimal growth of kelp in the Kriegers Flak area, driven by the low salinity of the Baltic Sea.

"Funded by the European Union, grant agreement NO 101094065. Views and opinions expressed are however those of the author(s) only and do not necessarily reflect those of the European Union or CINEA. Neither the European Union nor the granting authority can be held responsible for them."

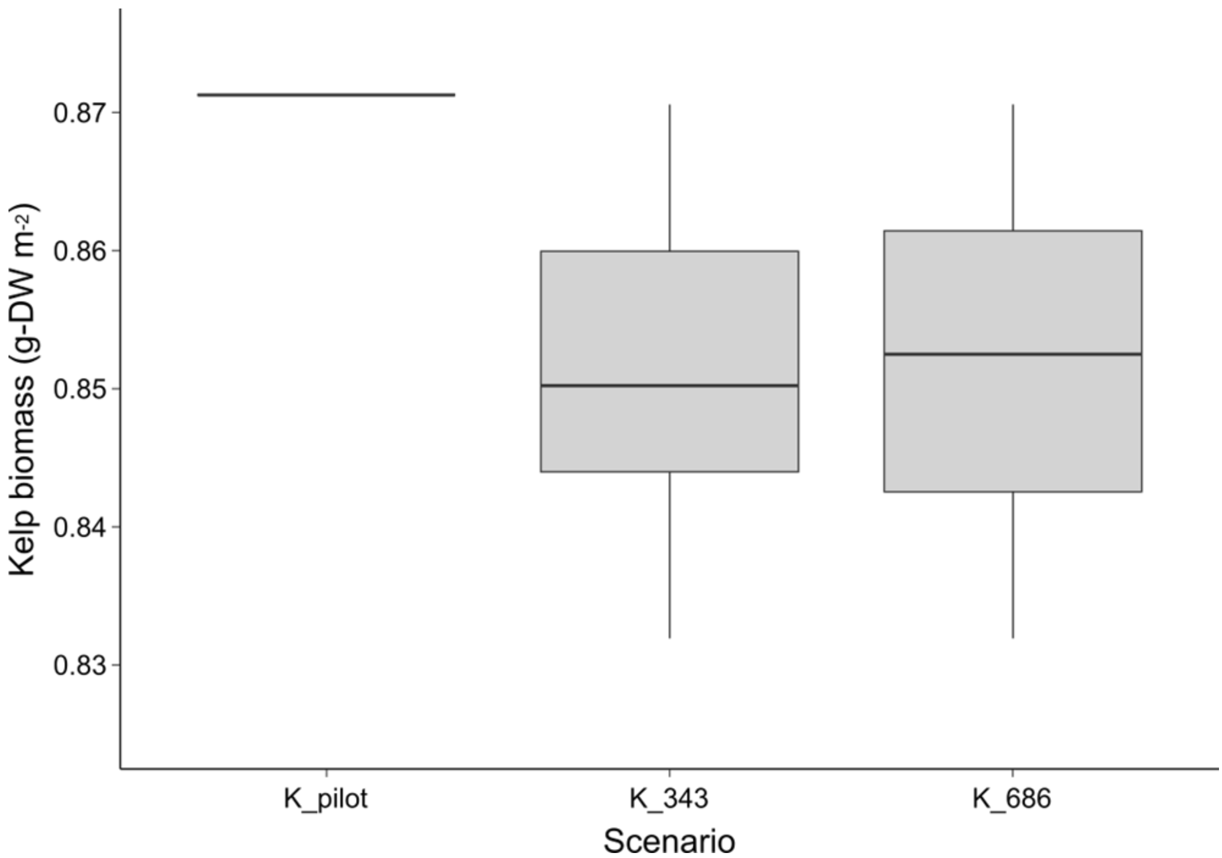

Figure 3.2.7. *Total kelp biomass (g-DW m^{-2}) for each farm at time of harvest (1st June) for scenarios K_pilot (single farm in pilot location), K_343 (42 farms placed 343 m distant from one another) and K_686 (22 farms placed 686 m distant from one another).*

3.2.3. Nutrients and carbon capture and water quality

Mussel farming

At the time of harvest (31st December) the amount of nitrogen present in mussel tissues, and therefore removed from the water column, from 2 – 5 m depth at the pilot farm location (M_pilot) was 73.55 g-N m^{-2} (Figure 3.2.8). Following the Redfield ratio for N:P, the total amount of phosphorous removed was therefore 4.60 g-P m^{-2}. The nitrogen, and therefore phosphorous, removed per individual farm at the time of harvest was greater in scenario M_686, where farms were placed 686 m distant from one another, than scenario M_343, where they were placed 343 m distant (Figure 3.2.8). This aligns with the greater mussel biomass observed in the M_686 scenario compared to the M_343 scenario (Figure 3.2.6). The same pattern was evident for the total carbon stored in the mussel shells (Figure 3.2.8), with 325.25 g-C m^{-2} at the pilot farm location (M_pilot) at the time of harvest (31st December). This would suggest that when placed too closely together reduced growth caused by depletion of food and nutrients limits the ecosystem services provided by mussel aquaculture.

"Funded by the European Union, grant agreement NO 101094065. Views and opinions expressed are however those of the author(s) only and do not necessarily reflect those of the European Union or CINEA. Neither the European Union nor the granting authority can be held responsible for them."

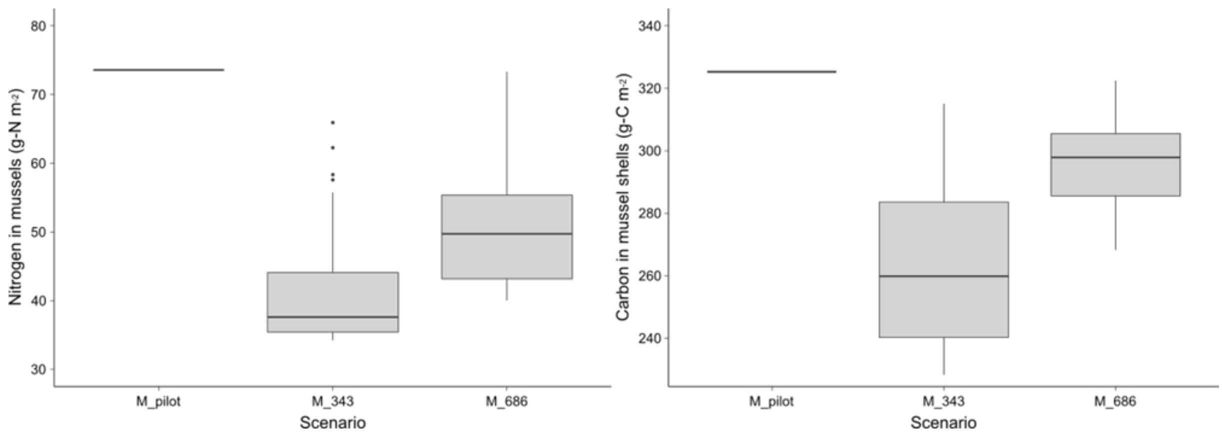

Figure 3.2.8. *(Left) Total nitrogen present in mussel tissues (g-N m^{-2}), and (Right) total carbon present in mussel shells (g-C m^{-2}) for each farm at time of harvest (31st December) for scenarios M_pilot (single farm in pilot location), M_343 (42 farms placed 343 m distant from one another) and M_686 (22 farms placed 686 m distant from one another).*

At the time of harvest (31st December) the greatest change in water clarity, measured as percentage difference from the reference scenario with no feedbacks to the biogeochemical model, used in the screening process, was observed in the M_343 scenario, where farms were placed 343 m distant from one another (Figure 3.2.9). Within a 1 km radius of farm locations in this scenario, there was an average reduction in Chl *a* of 32.7%, whilst for the M_686 scenario the average reduction in Chl *a* was 26.4%. This is likely due to the greater number of mussels present in this scenario, which despite their lower overall biomass (Figure 3.2.7) take up more phytoplankton, and therefore remove more Chl *a*, than the pilot or M_686 scenarios.

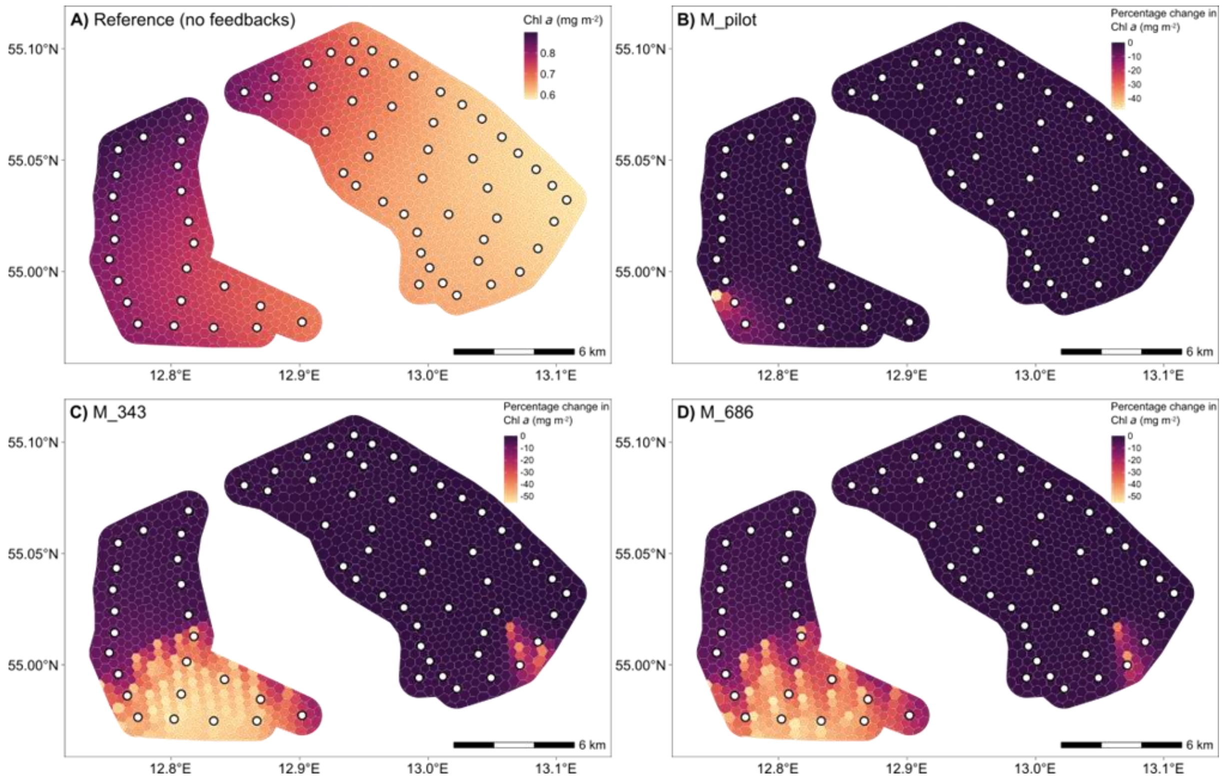

Figure 3.2.9. Spatial differences in water clarity at the surface for the different mussel farming scenarios, measured as percentage difference in Chlorophyll *a* from the reference screening scenario in which there were no feedbacks from the mussel model to the biogeochemical model. A) Surface Chl *a* (mg Chl *a* m^{-2}) in the reference screening scenario; B) Percentage change in Chl *a* in the M_pilot scenario (single farm in pilot location); C) Percentage change in Chl *a* in the

"Funded by the European Union, grant agreement NO 101094065. Views and opinions expressed are however those of the author(s) only and do not necessarily reflect those of the European Union or CINEA. Neither the European Union nor the granting authority can be held responsible for them."

M_343 scenario (42 farms placed 343 m distant from one another); D) Percentage change in Chl *a* in the M_686 scenario (22 farms placed 686 m distant from one another).

Kelp farming

At the time of harvest (1st June) the amount of nitrogen present in kelp, and therefore removed from the water column, from 0 – 6 m depth at the pilot farm location (K_pilot) was 0.011 g-N m^{-2} (Figure 3.2.10). Following the Redfield ratio for N:P, the total amount of phosphorous removed was therefore 0.00067 g-P m^{-2}. The nitrogen, and therefore phosphorous, removed per individual farm at the time of harvest was marginally greater in scenario K_686, where farms were placed 686 m distant form one another, than scenario K_343, where they were placed 343 m distant (Figure 3.2.10). This aligns with the slightly greater biomass observed in the K_686 scenario than the K_343 scenario. The same pattern was evident for the total carbon present in kelp (Figure 3.2.10), with 0.28 g-C m^{-2} at the pilot farm location (K_pilot) at the time of harvest (1st June). Overall, the low biomass growth caused by low salinity in the Baltic Sea and the Kriegers Flak area limits the ecosystem services kelp can provide, regardless of the number or spacing of aquaculture farms.

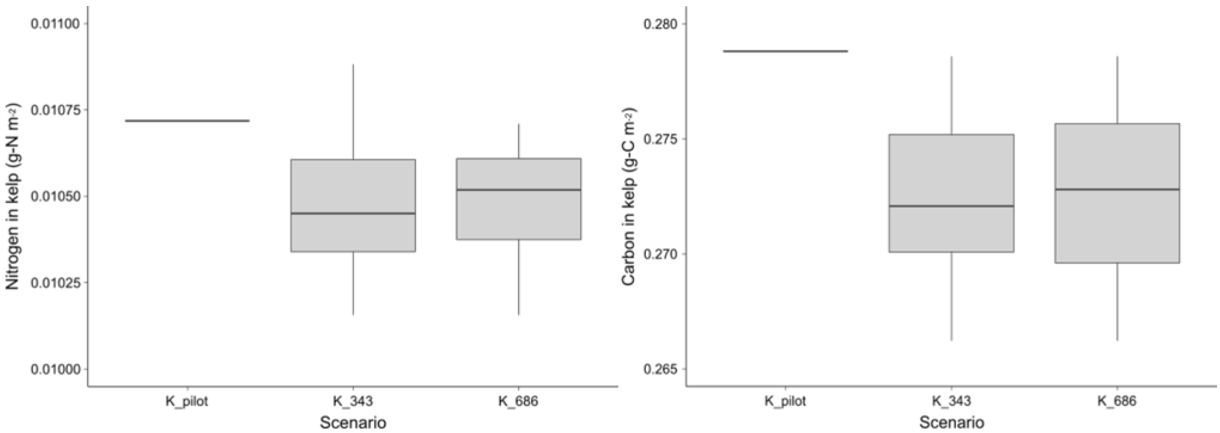

Figure 3.2.9. *(Left) Total nitrogen contained within kelp (g-N m^{-2}), and (Right) total carbon contained within kelp (g-C m^{-2}) for each farm at time of harvest (1st June) for scenarios K_pilot (single farm in pilot location), K_343 (42 farms placed 343 m distant from one another) and K_686 (22 farms placed 686 m distant from one another).*

3.3. Case C

3.3.1. Validation results

Rainbow trout and blue mussel model validation.

The results of the model validation for sea trout and blue mussel DEB models applied to Tagalaht bay are published in Kotta et al. 2022. The last blue mussel model incorporating the mechanistic approach for shell carbon deposition was validated and published in Vaher et al. 2024.

Fucus model validation

The *fucus* model performed well during the summer season, slightly underestimating growth during the colder spring months, and did not account for grazing losses starting mid-August (Figure 4.3.1). More data should make possible to further develop the nutrient and environmental impact on the growth and productivity described by the model. However, the cultivation method in cages within an IMTA system results in data where the interaction with

"Funded by the European Union, grant agreement NO 101094065. Views and opinions expressed are however those of the author(s) only and do not necessarily reflect those of the European Union or CINEA. Neither the European Union nor the granting authority can be held responsible for them."

other crops (blue mussel, competing algae) and variable grazing and complex shading effect produce large uncertainties. As such data from 2025 crop was not usable for further calibration.

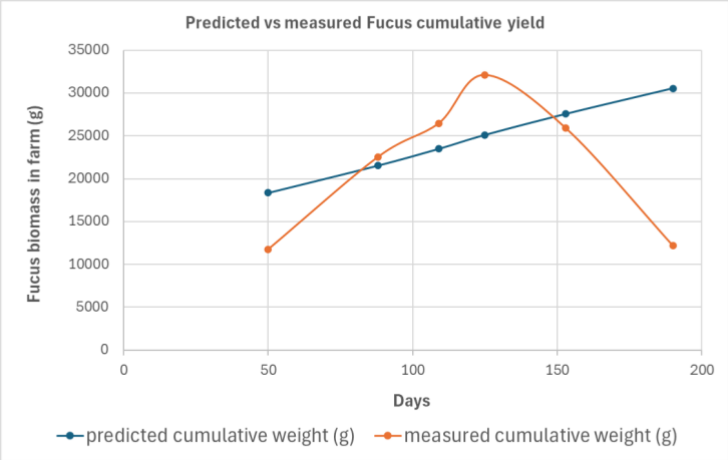

Figure 3.3.1. *Model comparison of Fucus growth with measurements over time.*

3.3.2. Growth and productivity results

In this study case there is only one scenario run for each species, corresponding with the set-up running at the pilot. More specifically for each farm/species: Finfish farming is fed farming and for the simulation we used the characteristics of the selected fish feed pellets to assess the fluxes of nutrients between the farm and the environment. Farm set-up was done using a realistic density with 70000 individuals and the simulations were run from the 1st of May to 21st of October. This is the production cycle at the area (Figure 3.3.2)

"Funded by the European Union, grant agreement NO 101094065. Views and opinions expressed are however those of the author(s) only and do not necessarily reflect those of the European Union or CINEA. Neither the European Union nor the granting authority can be held responsible for them."

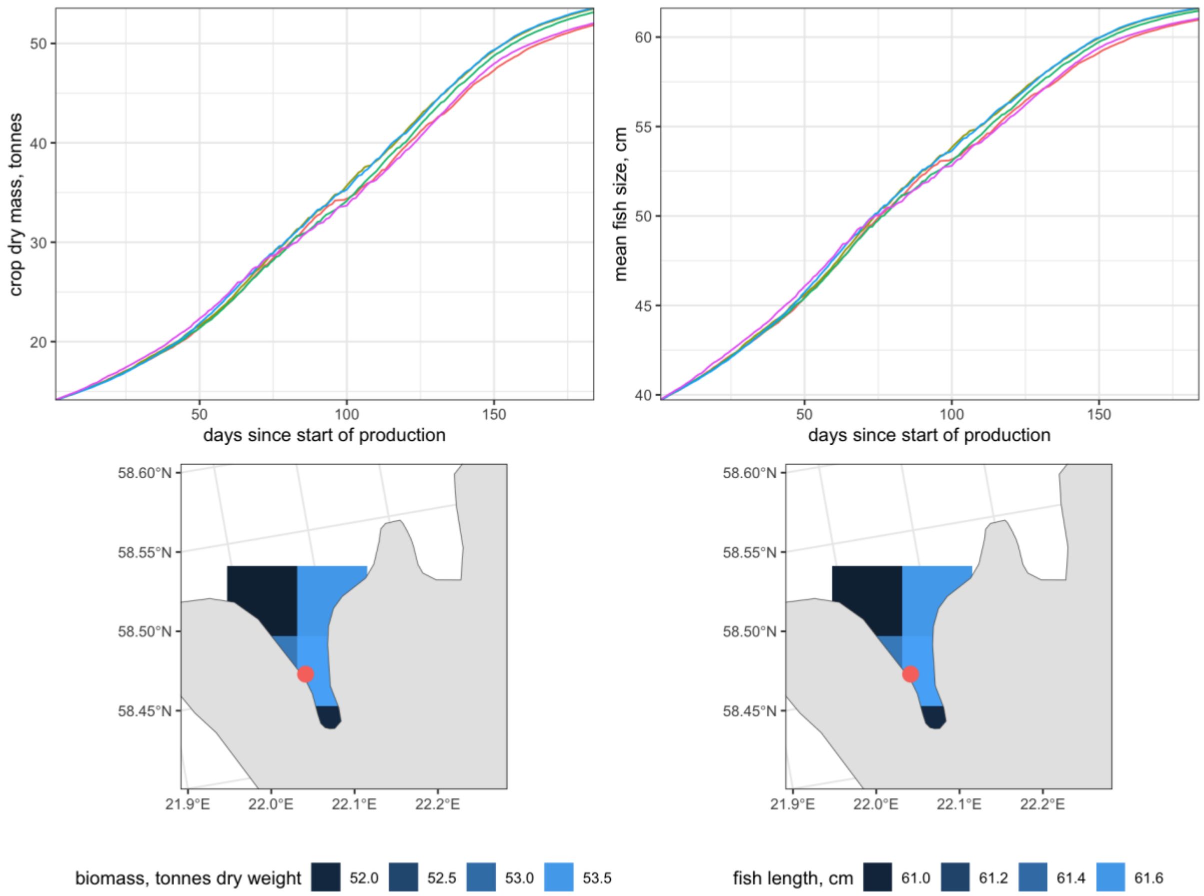

Figure 3.3.2. *Rainbow trout growth and biomass production (on the same farm setting) at Tagalaht bay. Each line in the top row plots represent one of the grid cells showing in the bottom maps. Orange dot in map shows the multiuse pilot location.*

For the blue mussel, the model was run under a realistic scenario involving a test farm with a population of 40 million individuals, distributed across six 100-meter-long lines. Blue mussel farms were run from 1st of June to the 21st of October of a year later (Figure 4.3.3). In this study case no differentiation is made between mitigation and human consumption mussels, that is because obtaining commercial size mussels is not feasible in this site due to low salinity.

"Funded by the European Union, grant agreement NO 101094065. Views and opinions expressed are however those of the author(s) only and do not necessarily reflect those of the European Union or CINEA. Neither the European Union nor the granting authority can be held responsible for them."

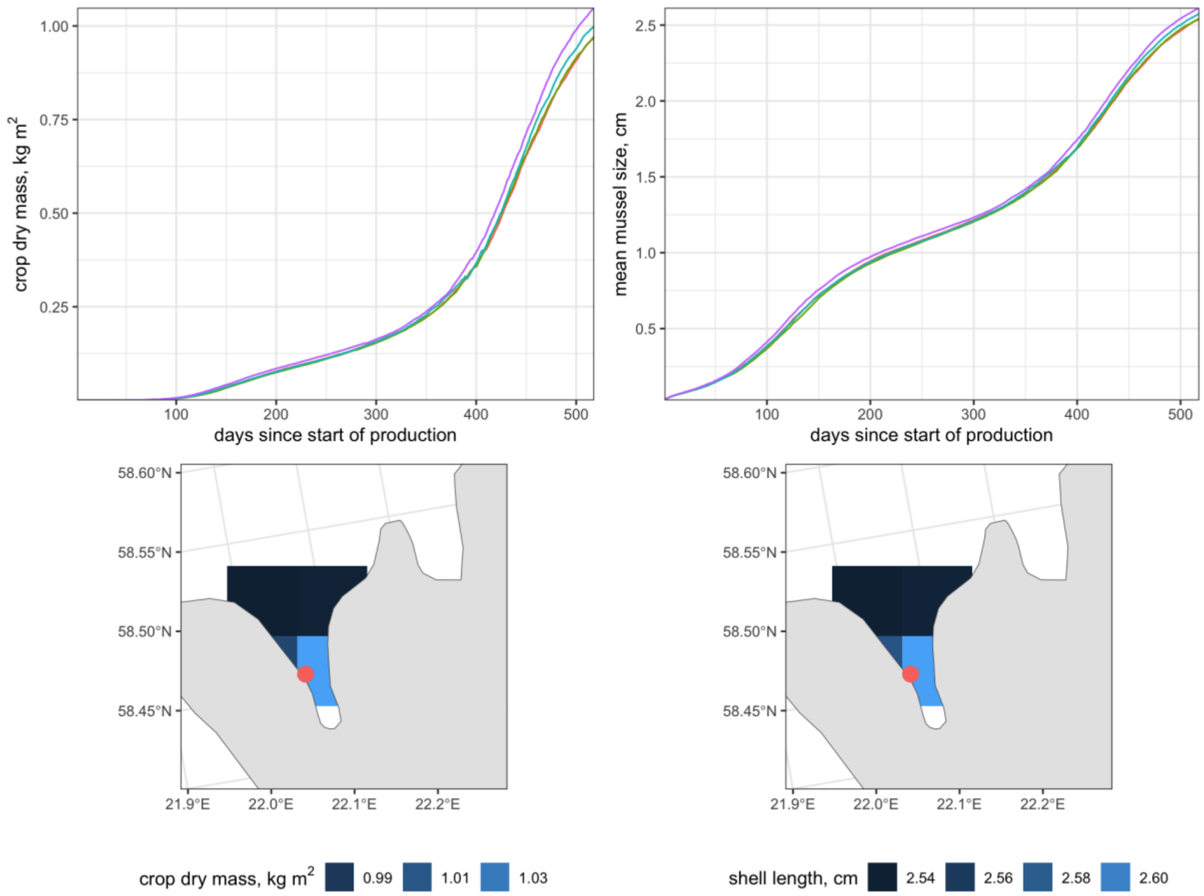

Figure 3.3.3. *Mussel production potential (DW per m²) and growth in shell length (on the same farm setting) at Tagalaht bay. Each line in the top row plots represent one of the grid cells showing in the bottom maps.*

The *Fucus* model was applied to a *Fucus* production set-up consisting of one net cage with a surface area of 6 m². An initial biomass of 10 kg of DW of algae is used in the modelling scenario. Simulation takes place from April to October (Figure 4.3.4).

"Funded by the European Union, grant agreement NO 101094065. Views and opinions expressed are however those of the author(s) only and do not necessarily reflect those of the European Union or CINEA. Neither the European Union nor the granting authority can be held responsible for them."

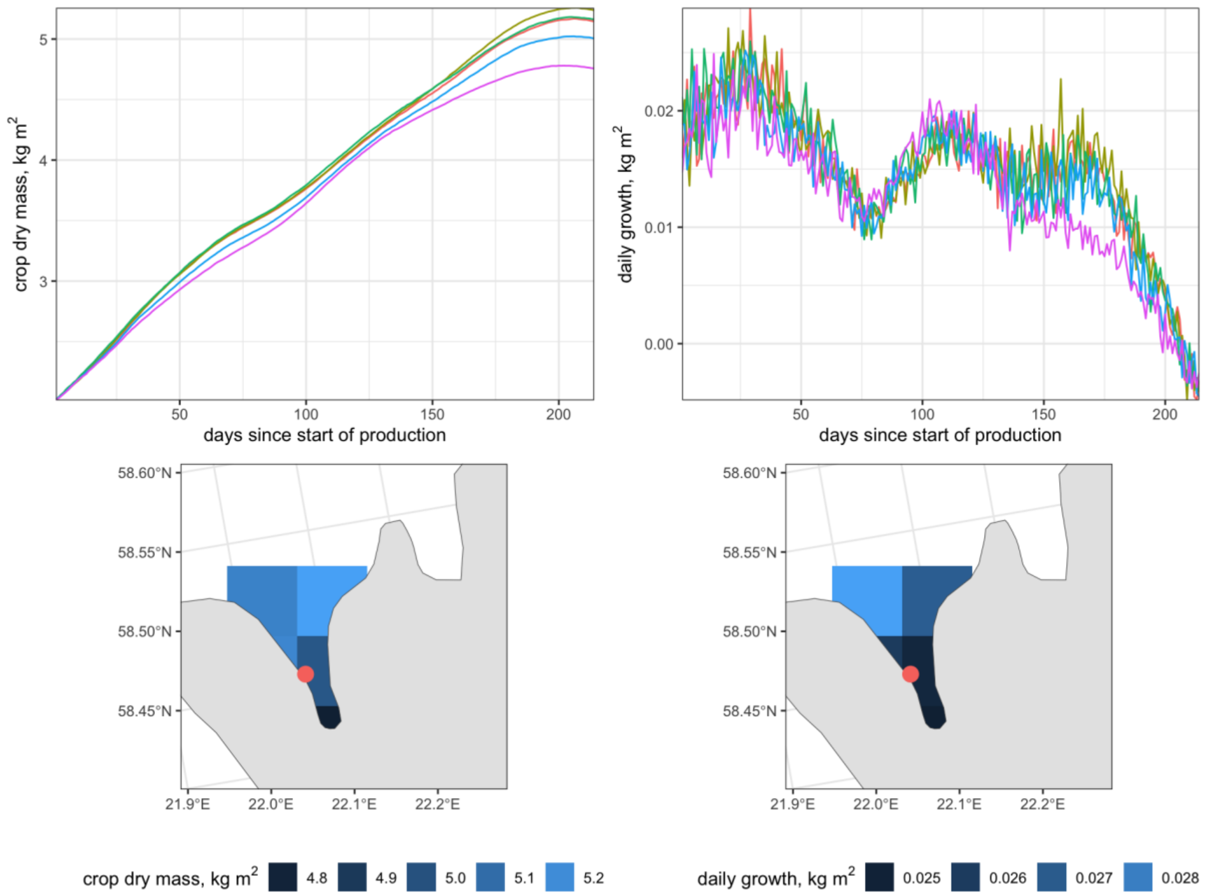

Figure 3.3.4. *Macroalgae production potential (DW per m^2) and daily growth (on the same farm setting, one cage of 6m^2) at Tagalaht bay. Each line in the top row plots represent one of the grid cells showing in the bottom maps.*

3.3.3. Nutrients and carbon capture and water quality

Mussel farming

Tagalaht Bay is located in the inner–central Baltic Sea, where salinity is low (5.5–6.5) and nutrient and chlorophyll *a* fluxes to the farm are modest (Chl *a* flux ca. 0.02–0.05 mg m^{-2} s^{-1}). Under these conditions, the modelled 0.25 ha mussel farm (about 40 million individuals) still attains a relatively high harvest of 950–1110 g DW m^{-2} over a 17-month cycle, corresponding to roughly 2.4–2.8 t DW per farm. At harvest, the mussels contain 215–252 g N m^{-2} and 25–28 g P m^{-2}, implying removal of about 0.54–0.63 t N and 0.06–0.07 t P per farm and production cycle. These values reflect assimilation of both background nutrients and the additional nutrient supply from the adjacent finfish cages.

The model also indicates substantial shell-bound carbon capture. Carbon contained in shells at harvest is 1615–1887 g C m^{-2}, equivalent to approximately 4.0–4.7 t C per 0.25 ha farm. This relatively high shell-carbon yield per unit area is consistent with pan-Baltic DEB modelling, which shows that in low-salinity inner and central regions, slow somatic growth and small mussel size increase the shell-to-tissue ratio and thus the importance of shell biocalcification for carbon capture (Vaher et al., 2024). Although outer Baltic sub-basins support much higher absolute shell-carbon capture per farm, these Tagalaht results confirm that mussel farming in the central/eastern Baltic can contribute meaningfully to long-term carbon storage.

"Funded by the European Union, grant agreement NO 101094065. Views and opinions expressed are however those of the author(s) only and do not necessarily reflect those of the European Union or CINEA. Neither the European Union nor the granting authority can be held responsible for them."

From a eutrophication-mitigation perspective, the Tagalaht nutrient removals are of the same order of magnitude as those predicted by Baltic-wide DEB applications for standard 0.25 ha farms (typically a few 10^2 kg N and a few 10^1 kg P per cycle; Kotta et al., 2023). However, regional modelling suggests that fully compensating the dissolved nutrient emissions of a medium-sized finfish farm in favourable western locations would require mussel farm areas on the order of several hectares (Kotta et al., 2023).

Given that the Tagalaht mussel farm is only 0.25 ha, the present configuration can only partially offset fish-farm nutrient discharges, although it still removes hundreds of kilograms of nitrogen per cycle and thus reduces net nutrient loading from this eutrophication hotspot. Because the Tagalaht simulations are based on single-box farm runs without feedback to a coupled biogeochemical model, changes in chlorophyll *a* and water clarity at the bay scale cannot yet be quantified. Nevertheless, the modelled food fluxes and filtration rates indicate that mussel farming is expected to exert a local top-down control on phytoplankton similar to that simulated for the more dynamic 3D cases, leading to improved water clarity in the immediate farm surroundings.

Fucus farming

The Tagalaht seaweed component consists of a single cage (6 m^2 surface area) stocked with 10 kg DW of *Fucus vesiculosus* and cultivated from April to October. First modelling results show very high areal biomass at harvest (4800–5200 g DW m^{-2}), which translates to about 29–31 kg DW per cage. The harvested biomass contains 1728–2184 g C m^{-2} (≈10–13 kg C per cage), 240–572 g N m^{-2} (≈1.4–3.4 kg N per cage) and 2.4–20 g P m^{-2} (≈15–120 g P per cage), assuming tissue stoichiometry derived from North Baltic *Fucus* analyses. Although these numbers refer to a small experimental unit, they indicate that, if scaled up, *Fucus* cultivation in Tagalaht could remove additional dissolved inorganic nitrogen and phosphorus from the water column and store several kilograms of carbon per cultivation module each year.

Baltic-wide macroalgal modelling has shown that *F. vesiculosus* farms have the highest nutrient-removal potential in moderately enriched coastal and offshore areas of the central and northern Baltic Sea, including the Gulf of Finland. In such settings, a single *Fucus* or *Ulva* farm can remove up to a few kilograms to tens of kilograms of nutrients per growth season and may reduce available nutrient stocks within a surrounding 1 km^2 area by up to ~0.15–0.30 % (Kotta et al., 2022). Thus, seaweed farms in the central/eastern Baltic Sea can make a measurable, though modest, contribution to nutrient reduction at the scale of small embayment, especially when deployed near existing point sources.

In Tagalaht, mussels and *Fucus* target complementary nutrient pools: mussels primarily remove particulate organic matter and associated nutrients via filtration and shell growth, whereas *Fucus* takes up dissolved inorganic nutrients during the productive season. Together, the modelled mussel farm and *Fucus* cage remove on the order of 10^2–10^3 kg N and several 10^1 kg P per cycle, while storing several tonnes of carbon in shells and additional kilograms of carbon in seaweed biomass. Although the current farm areas are too small to fully mitigate fish-farm emissions, these first results demonstrate that integrated low-trophic aquaculture in the central/eastern Baltic can contribute to nutrient and carbon management in eutrophic coastal

"Funded by the European Union, grant agreement NO 101094065. Views and opinions expressed are however those of the author(s) only and do not necessarily reflect those of the European Union or CINEA. Neither the European Union nor the granting authority can be held responsible for them."

systems and provide a basis for designing larger-scale IMTA configurations in Tagalaht and similar bays.

4. Summary

Ecosystem models coupled with low trophic aquaculture models (mussels and seaweed) were developed and validated against available measurements at the three OLAMUR case study sites. The models were applied to estimate the potential harvest (food provisioning) and ecosystem services related to the biological activity of the cultivated low trophic species in the environment. This model runs were used to provide data sets for other WPs, specifically data on production potential and ecosystem services will be used by WP2 micro sitting and ODSS tools and by WP5 Farm Performance Protocol module. The sites varied in environmental properties with highest salinity at site A in the German Bight, and very low salinity in the Baltic Sea at site B (Kriegers Flak) and C (Tagalaht bay). Fluxes of Chl *a* and nutrients supplying the aquaculture farms were highest in the German Bight followed by Kriegers Flak, and Tagalaht bay (Tables 5.1 and 5.2).

Blue mussels could be produced at each site (Table 5.1). Mussel growth is a key parameter determining the food provisioning ecosystem service. The mussel farm at site C is already well established and production has been optimized to achieve a high harvest of 1000 g-DW m^{-2} despite the low salinity and slow growth, they produce high biomass of small individuals, while they may not be optimal for human consumption due to their small size it is still a considerable biomass production. The pilot farm at site B showed a potential harvest of 450 to 700 g-DW m^{-2} depending on the distance between farms due to depletion of chlorophyll, similarly to pilot C production seems to be of smaller individuals (~2.5cm shell length). The higher salinity and food supply in Pilot A in the North Sea translates into a high production potential with production ranging from 3200 to 5300 g-DW m^{-2} of larger mussels, more appropriate for their use as human food.

Sugar kelp was found to be very sensitive to low salinity showing low growth rates and farming must be considered unsuitable for Kriegers Flak based on both measurements and modelling. It would probably be more ideal to grow sugar kelp at higher salinities, e.g., offshore at site A in the German Bight (Table 5.2).

Fucus showed the highest harvest potential among the tested species and will be worth cultivating. This represents the first successful case of seaweed cultivation in the low-salinity environment of the Baltic Sea. The only challenge was the strong grazing on *Fucus* observed later in the season, which could be managed with proper strategies. More data is also necessary to improve the production model.

As expected, both mussels and the different species of seaweed have a high capacity to capture nutrients and carbon. However, these capabilities depend on the production potential of the region (Table 5.1 and 5.2). Regarding the mussels, the more efficient cultivation the higher capacity to harvest nitrogen and phosphorous. In the pilots A and B the models can be used to

"Funded by the European Union, grant agreement NO 101094065. Views and opinions expressed are however those of the author(s) only and do not necessarily reflect those of the European Union or CINEA. Neither the European Union nor the granting authority can be held responsible for them."

evaluate this harvest of nutrients and removal depending on the aquaculture intensity allowing for optimisation of the location and cultivation load and to determine the carrying capacity of the activity. When focusing in the shell carbon capture the Site C is the more efficient, this is the result of slow growing mussels at low salinities. Site C can produce a large biomass of mussels, but the average mussel size is small (~2.5cm shell length) which results in a higher ratio shell to tissue (Table 5.1). The mussel grazing impact on the phytoplankton is also reflected in the water clarity improvement due to cultivation.

Table 5.1. *Summary of the mussel model estimates of salinity, Chl a fluxes and mussel harvest potential (DW, C, N and P) at the three sites. * calculated applying the DEB standard chemical composition of tissues (Kooijman 2010).*

	Site A German Bight	Site B Kriegers Flak	Site C Tagalaht bay
Salinity (psu)	29.7-34.3	7.5-8.5	5.5-6.5
Chl a flux (mg-m^{-2} s^{-1})	0.80-1.31	0.17-0.30	0.02-0.05
Mussel harvest (g-DW m^{-2})	3200-5300	360-811	950-1110
Carbon shell harvest (g-C m^{-2})	-	228-326	1615-1887
Nitrogen harvest (g-N m^{-2})	560-927*	34-74	215-252
Phosphorus harvest (g-P m^{-2})	-	2.1-4.6	25-28
Average % change in water clarity (mg Chl *a* m^{-2}) within a 1 km radius of farms	-0.1%-12.4%	-11.5%-32.7%	-

Nutrient harvested by seaweed production follows the same pattern. As a result the potential of sugar kelp in the site B to harvest nutrients is extremely low due to their poor growth. Meanwhile the successful production of *Fucus* in the site C shows a high protential to be used on nutrient mitigation strategies, or nutrient harvest (Table 5.2.)

Table 5.2. *Summary of the seaweed model estimates of nutrient fluxes and seaweed harvest potential at the three sites. * Estimates from Fucus harvest based on Takolander, 2018 tissue analyses in the North Baltic sea.*

	Site A German Bight	Site B Kriegers Flak	Site C Tagalaht bay
Nitrogen flux (mmol m^{-2} s^{-1})	-	0.8-1.1	0.1-0.3
Sugar kelp harvest (g-DW m^{-2})	-	0.83-0.88	-
***Fucus* harvest (g-DW m^{-2})**	-	-	4800-5200
Carbon harvest (g-C m^{-2})	-	0.26-0.28	1728-2184*
Nitrogen harvest (g-N m^{-2})	-	0.01-0.011	240-572*
Phosphorus harvest (g-P m^{-2})	-	0.0006-0.0007	2.4 – 20*

Overall, the use of modelling approaches such as the ones applied here demonstrate the potential of the use of co-location for cultivation of low trophic species and their use to provide a sustainable food resource and to be used in environmental mitigation strategies. The models applied in the OLAMUR pilots can be used to assess the ecosystem services of LTA activities in multi-use offshore areas. In this task we have used these models to assess production potential, crop characteristics and other key quantities associated to biomass production such as the use of nutrients and chl-a by the different crops modelled. Such quantities can be used to

"Funded by the European Union, grant agreement NO 101094065. Views and opinions expressed are however those of the author(s) only and do not necessarily reflect those of the European Union or CINEA. Neither the European Union nor the granting authority can be held responsible for them."

evaluate the ecosystem services of these activities under a variety of production scenarios related to carrying capacity, location and production cycle.

The evaluation of ecosystem services using these model derived quantities is not straightforward. The impact of the crop in the environment and therefore the relevance of these quantities as ecosystem services relates mainly to the environmental conditions of the location and the overall performance of the crops. A clear example is the impact on the Chl-a concentration and water clarity, a regulating ecosystem service by mussels, when comparing pilot A and B the decrease of Chl-a concentration is especially significant in pilot B (Table 5.1) however the higher cultivated biomass in pilot A have a negligible impact in the Chl-a concentration patterns (Figure 3.1.8). A similar pattern is observed in the nutrient uptake by blue mussels and therefore their nutrient load mitigation capacity.

The main ecosystem service of low trophic aquaculture is the provisioning of food, cultivation of mussels in pilot A and *Fucus* in pilot C have a high potential producing large mussels and large biomass of algae. However, in Pilot B and C for mussel cultivation produces small mussels that are currently not being used by the food industry, therefore the capacity of using mussel aquaculture as food provisioning service is currently low. Contrasting, these locations offer the higher capacity for mussels to be used for their regulating ecosystem services as they have a higher impact on water clarity, nutrient removal and carbon capture per biomass produced. Nutrient regulation in Pilot C has been shown to be important when linked to fin fish cultivation (Kotta et al. 2020), and in Denmark coastal waters (Maar et al. 2023).

The capacity of LT species to regulate inorganic carbon in seawater is complex. While macroalgae directly relate to CO_2 uptake and accumulation as organic carbon, the regulating impact of blue mussels calcification is more complex and the effect on local inorganic carbon chemistry relates to the uptake of bicarbonate and the release of CO_2, which results in a negative impact on acidification and overall capacity of these organisms to be used for carbon removal (Pernet et al. 2024)

"Funded by the European Union, grant agreement NO 101094065. Views and opinions expressed are however those of the author(s) only and do not necessarily reflect those of the European Union or CINEA. Neither the European Union nor the granting authority can be held responsible for them."

5. References.

Boderskov T., Rasmussen M.B., & Bruhn A. (2023). Upscaling cultivation of *Saccharina latissima* on net or line systems; comparing biomass yields and nutrient extraction potentials. *Frontiers in Marine Science, 10*. https://doi.org/10.3389/fmars.2023.992179

Broch O.J., & Slagstad D. (2012). Modelling seasonal growth and composition of the kelp *Saccharina latissima*. *Journal of Applied Phycology, 24*, p. 759-776. https://doi.org/10.1007/s10811-011-9695-y

Bruhn A., Tørring D.B., Thomsen M., Canal-Vergés P., Nielsen M.M., Rasmussen M.B., Eybye K.L., Larsen M.M., Balsby T.J.S., & Petersen J.K. (2016). Impact of environmental conditions on biomass yield, quality, and bio-mitigation capacity of *Saccharina latissima*. *Aquaculture Environment Interactions, 8*, p. 619-636. https://doi.org/10.3354/aei

Buer, A-L., Maar, M., Nepf, M., Ritzenhofen, L., Dahlke, S., Friedland, R., Krost, P., Peine, F., & Schernewski, G. (2020). Potential and feasibility of *Mytilus* spp. farming along a salinity gradient. *Frontiers of Marine Science*, *7*. https://doi.org/10.3389/fmars.2020.00371

Bruggeman, J., and Bolding, K. (2014). A general framework for aquatic biogeochemical models. *Environmental modelling and software*, *61*, 249-265. https://doi.org/10.1016/j.envsoft.2014.04.002

Chen, Z., Snow, M., Lawrence, C. S., Church, A. R., Narum, S. R., Devlin, R. H., Farrell, A. P. (2015); Selection for upper thermal tolerance in rainbow trout (*Oncorhynchus mykiss* Walbaum). *Journal Experimental Biology*; 218 (5): 803–812. https://doi.org/10.1242/jeb.113993

Daewel, U., and Schrum, C. (2013). Simulating long-term dynamics of the coupled North Sea and Baltic Sea ecosystem with ECOSMO II: Model description and validation. *Journal of Marine Systems*, *119*, 30-49. https://doi.org/10.1016/j.jmarsys.2013.03.008

Davidson, J. W., Kenney, P. B., Manor, M., Good, C. M., Weber, G. M., Aussanasuwannakul, A., Turk, P. J., Welsh, C., and Summerfelt, S. T. (2014). Growth performance, fillet quality, and reproductive maturity of rainbow trout (*Oncorhynchus mykiss*) cultured to 5 kilograms within freshwater recirculating systems. *Journal of Aquaculture Research and Development*, 5(4). https://doi.org/10.4172/2155-9546.1000238

Duteil, O., Macias Moy, D., & Stips, A. (2023). Sensitivity of the North Sea ecosystem to a combined reduction of phosphorus and nitrogen loads: A model study (Report No. JRC 132207). Publications Office of the European Union. https://publications.jrc.ec.europa.eu/repository/bitstream/JRC132207/JRC132207_01.pdf

From, J., & Rasmussen, G. (1991). Growth of rainbow trout, *Oncorhynchus mykiss* (Walbaum, 1792) related to egg size and temperature. *Dana,* 9, 31-38.

Hersbach, H., Bell, B., Berrisford, P., Hirahara, S., Horányi, A., Muñoz-Sabater, J., ... & Thépaut, J. N. (2020). The ERA5 global reanalysis. *Quarterly journal of the royal meteorological society*, *146*(730), 1999-2049. https://doi.org/10.1002/qj.3803

Holst N., Boderskov T., Bruhn A. (2025). A simple growth model of *Saccharina latissima* cultivated in Scandinavia: Theoretical and practical implications. *Algal Research, 87*. https://doi.org/10.1016/j.algal.2025.103971

"Funded by the European Union, grant agreement NO 101094065. Views and opinions expressed are however those of the author(s) only and do not necessarily reflect those of the European Union or CINEA. Neither the European Union nor the granting authority can be held responsible for them."

Hosseini, S. T., Pein, J., Staneva, J., Zhang, Y. J., & Stanev, E. (2025). Impact of offshore wind farm monopiles on hydrodynamics interacting with wind-driven waves. *Ocean Modelling*, *195*, 102521.

Jevne L.S., Forbord S., & Olsen Y. (2020). The Effect of Nutrient Availability and Light Conditions on the Growth and Intracellular Nitrogen Components of Land-Based Cultivated *Saccharina latissima* (Phaeophyta). *Frontiers in Marine Science, 7*. https://doi.org/10.3389/fmars.2020.557460

Kieffer, J. D., Alsop, D., and Wood, C. M. (1998). A respirometric analysis of fuel use during aerobic swimming at different temperatures in rainbow trout (*Oncorhynchus mykiss*). *Journal of Experimental Biology*, 201(22):3123—3133

Kotta, J., Orav-Kotta, H. and Vuorinen, I. (2005). Field measurements on the variability in biodeposition and grazing pressure of suspension feeding bivalves in the northern Baltic Sea. In: R. Dame & S. Olenin (eds) The Comparative Roles of Suspension Feeders in Ecosystems. Springer, The Netherlands, Dordrecht, pp. 11–29.

Kotta, J., Futter, M., Kaasik, A., Liversage, K., Rätsep, M., Barboza, F. R., Bergström, L., Bergström, P., Bobsien, I., Díaz, E., Herkül, K., Jonsson, P. R., Korpinen, S., Kraufvelin, P., Krost, P., Lindahl, O., Lindegarth, M., Lyngsgaard, M. M., Mühl, M., … Virtanen, E. (2020). Cleaning up seas using blue growth initiatives: Mussel farming for eutrophication control in the Baltic Sea. *Science of the Total Environment*, 709, 136144.

Kotta, J., Raudsepp, U., Szava Kovats, R., Aps, R., Armoskaite, A., Barda, I., … Barboza, F. R. (2022). Assessing the potential for sea based macroalgae cultivation and its application for nutrient removal in the Baltic Sea. *Science of the Total Environment*, 839, 156230. https://doi.org/10.1016/j.scitotenv.2022.156230

Kotta, J.; Stechele, B.; Barboza, F.R.; Kaasik, A.; Lavaud, R. 2023. Towards environmentally friendly finfish farming: A potential for mussel farms to compensate fish farm effluents. *Journal of Applied Ecology,* 60, 1314–1326. https://doi.org/10.1111/1365-2664.14422

Kooijman, S. A. L. M. (2010). Dynamic Energy Budget theory for metabolic organisation (Third). Cambridge University Press.

Larsen, P. S., Lundgreen, K., & Riisgård, H. U. (2013). Bioenergetic model predictions of actual growth and allometric transitions during ontogeny of juvenile blue mussels *Mytilus edulis*. *Mussels: Ecology, Life Habits and Control; Nowak, J., Kozlowski, M., Eds*, 101-122.

Larsen J. (2024). FlexSem source code. *Zenodo*. https://doi.org/10.5281/zenodo.13268690

Larsen J., Mohn C., Pastor A., & Maar M. (2020). A versatile marine modelling tool applied to arctic, temperate and tropical waters. *PLoS ONE, 15*(4), e0231193. https://doi.org/10.1371/journal.pone.0231193

Lauff, R. F. and Wood, C. M. (1996). Respiratory gas exchange, nitrogenous waste excretion, and fuel usage during starvation in juvenile rainbow trout*, Oncorhynchus mykiss*. *Journal Comparative Physiology, Part B*, 165:542--551.

Lauringson, V., Kotta, J., Orav-Kotta, H., Kotta, I., Herkül, K. and Põllumäe, A. (2009). Comparison of benthic and pelagic suspension feeding in shallow water habitats of the northeastern Baltic Sea. *Marine Ecology*, 30, 43–55.

"Funded by the European Union, grant agreement NO 101094065. Views and opinions expressed are however those of the author(s) only and do not necessarily reflect those of the European Union or CINEA. Neither the European Union nor the granting authority can be held responsible for them."

Maar, M., Bolding, K., Petersen, J. K., Hansen, J. L., and Timmermann, K. (2009). Local effects of blue mussels around turbine foundations in an ecosystem model of Nysted off-shore wind farm, Denmark. *Journal of Sea Research*, *62*(2-3), 159-174. https://doi.org/10.1016/j.seares.2009.01.008

Maar, M., Larsen, J., Schourup-Kristensen, V., & Taylor, D. (2023). Nutrient extraction and ecosystem impact by suspended mussel mitigation cultures at two contrasting sites. *Science of the Total Environment*, *888*. https://doi.org/10.1016/j.scitotenv.2023.164168

Maar, M., Larsen, J., Butenschön, M., Kristiansen, T., Thodsen, H., Taylor, D., & Schourup-Kristensen, V. (2024). Impacts of climate change on water quality, benthic mussels, and suspended mussel culture in a shallow, eutrophic estuary. *Heliyon*, *10*(3). https://doi.org/10.1016/j.heliyon.2024.e25218

Nielsen M.M., Manns D., D'Este M., Krause-Jensen D., Rasmussen M.B., Larsen M.M., Alvarado-Morales M., Angelidaki I., & Bruhn A. (2016). Variation in biochemical composition of *Saccharina latissima* and *Laminaria digitata* along an estuarine salinity gradient in inner Danish waters. *Algal Research, 13*, p. 235-245. https://doi.org/10.1016/j.algal.2015.12.003

Ninness, M. M., Stevens, E. D., and Wright, P. A. (2006). Removal of the chorion before hatching results in increased movement and accelerated growth in rainbow trout (*Oncorhynchus mykiss*) embryos. *Journal of Experimental Biology*, 209(10):1874--1882.

Pein, J., Eisele, A., Sanders, T., Daewel, U., Stanev, E. V., Van Beusekom, J. E., Staneva, J. and Schrum, C. (2021). Seasonal stratification and biogeochemical turnover in the freshwater reach of a partially mixed dredged estuary. *Frontiers in Marine Science*, *8*, 623714. https://doi.org/10.3389/fmars.2021.623714

Pein, J., Staneva, J., Mayer, B., Palmer, M. D., and Schrum, C. (2023). A framework for estuarine future sea-level scenarios: Response of the industrialised Elbe estuary to projected mean sea level rise and internal variability. *Frontiers in Marine Science*, *10*, 1102485. https://doi.org/10.3389/fmars.2023.1102485

Pein, J., Staneva, J. (2024). Eutrophication hotspots, nitrogen fluxes and climate impacts in estuarine ecosystems: A model study of the Odra estuary system. *Ocean Dynamics* **74**, 335–354. https://doi.org/10.1007/s10236-024-01607-w

Pernet F., Dupont S., Gattuso J.-P., Metian M., Gazeau F. (2024). Cracking the myth: Bivalve farming is not a CO2 sink. *Reviews in Aquaculture* 17(1):e12954. https://doi.org/10.1111/raq.12954

Petersen, J. K., & Loo, L. O. (2004). Miljøkonsekvenser af dyrking av blåmuslinger. Interregproject III-A "Blåskjellanlegg og nitrogenkvoter". Slutrapport, 31, 2004.

Radach, G., & Moll, A. (2006). Review of three-dimensional ecological modelling related to the North Sea shelf system. Part II: Model validation and data needs, in: Gibson, R. N., Atkinson, R. J. A., & Gordon, J. D. M. (Eds.), *Oceanography and Marine Biology. An Annual Review*, *44*, p. 1-60.

Rennau, H., Schimmels, S., & Burchard, H. (2012). On the effect of structure-induced resistance and mixing on inflows into the Baltic Sea: A numerical model study. *Coastal Engineering*, *60*, p. 53-68. https://doi.org/10.1016/j.coastaleng.2011.08.002

"Funded by the European Union, grant agreement NO 101094065. Views and opinions expressed are however those of the author(s) only and do not necessarily reflect those of the European Union or CINEA. Neither the European Union nor the granting authority can be held responsible for them."

Riisgård, H. U., Pleissner, D., Lundgreen, K., & Larsen, P. S. (2013). Growth of mussels *Mytilus edulis* at algal (*Rhodomonas salina*) concentrations below and above saturation levels for reduced filtration rate. *Marine Biology Research*, 9(10), 1005-1017.

Roberts, E.A. and Kooijman, B. (2019). AmP *Mytilus trossulus*, version 2019/03/16. https://www.bio.vu.nl/thb/deb/deblab/add_my_pet/entries_web/Mytilus_trossulus/Mytilus_trossulus_res.html

Roland, A., Zhang, Y. J., Wang, H. V., Meng, Y., Teng, Y. C., Maderich, V., ... & Zanke, U. (2012). A fully coupled 3D wave-current interaction model on unstructured grids. *Journal of Geophysical Research: Oceans*, *117*(C11).

Schrum, C., Alekseeva, I., and John, M. S. (2006). Development of a coupled physical–biological ecosystem model ECOSMO: part I: model description and validation for the North Sea. *Journal of Marine Systems*, *61*(1-2), 79-99. https://doi.org/10.1016/j.jmarsys.2006.01.005

Stavrakidis-Zachou, O., Papandroulakis, N., & Lika, K. (2019). A DEB model for European sea bass (Dicentrarchus labrax): Parameterisation and application in aquaculture. *Journal of Sea Research*, 143, 262–271.

Sumpter, J. P., le Bail, P. Y., Pickering, A. D., Pottinger, T. G., and Carragher, J. (1991). The effect of starvation on growth and plasma growth hormone concentrations of rainbow trout, *Oncorhynchus mykiss*. *General and Comparative Endocrinology*, 83:94--102.

Takolander, A. (2018). Assessing the effects of climate change on Baltic Sea macroalgae – implications for the foundation species *Fucus vesiculosus* L. PhD Thesis. Faculty of Biological and Environmental Sciences University of Helsinki. http://hdl.handle.net/10138/238810

Taylor, D., Larsen, J., Buer, A-L., Friedland, R., Holbach, A., Petersen, J. K., Nelsen, P., Ritzenhofen, P., Saurel, C., & Maar, M. (2021). Mechanisms influencing particle depletion in and around mussel farms in different environments. *Ecological Indicators*, *122*. https://doi.org/10.1016/j.ecolind.2020.107304

Tyler, C. R., Pottinger, T. G., Santos, E., Sumpter, J. P., Price, S.-A., Brooks, S., and Nagler, J. J. (1996). Mechanisms controlling egg size and number in the rainbow trout, *Oncorhynchus mykiss*. *Biology of reproduction,* 54:8--15.

Vaher, A., Kotta, J., Stechele, B., Kaasik, A., Herkül, K., & Barboza, F. R. (2024). Modelling and mapping carbon capture potential of farmed blue mussels in the Baltic Sea region. Science of the Total Environment, 947, 174613. https://doi.org/10.1016/j.scitotenv.2024.174613

Veber, T. (1998). Söödava rannakarbi, *Mytilus edulis* L. levikut ja populatsioonistruktuuri mõjutavad faktorid Lääne-eesti rannikumeres. BSc. thesis, University of Tartu.

Velsen, F. P. J. (1987). Temperature and incubation in Pacific salmon and rainbow trout: Compilation of data on median hatching time, mortality and embryonic staging. Technical Report 626, Canadian Data Report of Fisheries and Aquatic Science

Weatherly, A. H. and Gill, H. S. (1981). Recovery growth following periods of restricted rations and starvation in rainbow trout *Salmo gairdneri* Richardson.

"Funded by the European Union, grant agreement NO 101094065. Views and opinions expressed are however those of the author(s) only and do not necessarily reflect those of the European Union or CINEA. Neither the European Union nor the granting authority can be held responsible for them."

Wieser, W. (1985). Developmental and metabolic constraints of the scope for activity in young rainbow trout (*Salmo gairdneri*). Journal of Experimental Biology, 118(1):133--142.

Yanik, T., Hisar, S. A., and Bölükbas, C. (2002). Early development and growth of Arctic charr (*Salvelinus alpinus*) and rainbow trout (*Oncorhynchus mykiss*) at a low water temperature. The Israeli Journal of Aquaculture, 54(2):73

Zhang, Y. J., Ye, F., Stanev, E. V., and Grashorn, S. (2016). Seamless cross-scale modeling with SCHISM. *Ocean Modelling*, *102*, 64-81. https://doi.org/10.1016/j.ocemod.2016.05.002

Zollmann M., Rubinsky B., Liberzon A., & Golberg A. (2021). Multi-scale modeling of intensive macroalgae cultivation and marine nitrogen sequestration. *Communications Biology, 4*, 848. https://doi.org/10.1038/s42003-021-02371-z

"Funded by the European Union, grant agreement NO 101094065. Views and opinions expressed are however those of the author(s) only and do not necessarily reflect those of the European Union or CINEA. Neither the European Union nor the granting authority can be held responsible for them."